

Rolling Tines – Evaluation and Simulation Using
Discrete Element Method

By
Jay Mak

A thesis submitted to
the Faculty of Graduate Studies of the
University of Manitoba
in partial fulfilment of
the requirements of the degree of
Master of Science

Department of Biosystems Engineering
University of Manitoba
Winnipeg, Manitoba

© Copyright
2011, Jay Mak

**THE UNIVERSITY OF MANITOBA
FACULTY OF GRADUATE STUDIES**

COPYRIGHT PERMISSION

A Thesis/Practicum submitted to the Faculty of Graduate Studies of The University of
Manitoba in partial fulfillment of the requirement of the degree of
Master of Science in Engineering

©2011

Permission has been granted to the Library of the University of Manitoba to lend or sell copies of this thesis/practicum, to the National Library of Canada to microfilm this thesis and to lend or sell copies of the film, and to University Microfilms Inc. to publish an abstract of this thesis/practicum.

This reproduction or copy of this thesis has been made available by authority of the copyright owner solely for the purpose of private study and research, and may only be reproduced and copied as permitted by copyright laws or with express written authorization from the copyright owner.

General Abstract

Conservation tillage has been commonly practiced in recent times to offer soil protection from erosion and compaction, while conserving moisture and reducing energy cost. The rotary tine aerator combined with manure application is a conservational tillage implement that enhances manure infiltration into soils. The rotary tine aerator is a relatively new tillage tool with limited performance studies. The objectives of the study were to evaluate the soil disturbances and manure dispersion created by the AerWay aerator in a field with a silt loam soil; and to generate a calibrated and validated soil-tool model using Discrete Element Methods (DEM) that simulate the draft and vertical forces of the aerator. The variables examined were soil pocket size, pocket width, pocket depth, soil overthrown, and manure surface cover. The model predicted the draft force of the aerator and also offered predictions regarding the required vertical force for the aerator to puncture the soil.

The experimental results showed that a trend indicated that the faster tractor speeds would create larger pockets and minimize the amount of soil overthrown. At the manure application rate of 42 000 L/ha, manure was dispersed to a maximum depth of 250 mm, spread 200 mm in the forward direction and spread 100 mm in the lateral direction after one hour of application.

From the model results, the calibrated soil was found to have ball stiffness (k_n and k_s) of 10 kN/m and bond stiffness ($\overline{K_n}$ and $\overline{K_s}$) of 1 kPa/m with a relative error of 7.7% for a silt loam soil. The draft force from the model had a relative error of 13.4-31.2% when compared to the literature data between 100-150 mm depth. The predicted vertical force was found to linearly increase until the depth of 150 mm at around 700 N per rolling tine and plateaus until the full insertion of 200 mm. The correlation suggested that DEM modeling is a very promising method to simulate highly variable soil properties, nonlinear dynamic behaviour of soil, and complex phenomena of soil-tool interactions.

Acknowledgments

I would like to thank my supervisor, Dr. Ying Chen, for providing this opportunity as well as her excellent guidance throughout the project. I would like to thank the members of my graduate committee, Dr. Neil McLaughlin and Dr. Mark Tachie, for their continuous advice and comments. Special thanks to Dr. Sylvio Tessier for setting up and operating the tractor throughout the experiment. I would also like to thank a group of M.Sc. and Ph.D. students, Mr. Song Ai, Mr. Mohammed Al-Amin Sadek, Mr. Majibur Rahman Khan Mr. Jinke Xu and Mr. Klayton Kaleta, for their assistance on collecting the data from the field. Lastly, I would like to thank NSERC for funding this project and Biosystems Engineering Department at the University of Manitoba for the use of their facilities.

Table of Contents

Front Matter

Table of Contents.....	ii
List of Tables.....	v
List of Figures.....	vi
List of Symbols.....	viii
1 Introduction	1
1.1 General Objectives.....	4
1.2 Application of Modelling Tools.....	4
1.3 Understanding the Agricultural Practices	6
1.4 Model Evolution.....	6
1.5 Model Development.....	9
1.6 The Challenge – Comparison to Reality.....	10
1.7 Summary.....	11
2 Soil Disturbance and Liquid Manure Dispersion in Soil Resulting from a Rolling Tine Liquid Manure Applicator	12
2.1 Abstract.....	12
2.2 Introduction	13
2.2.1 Objectives	16
2.3 Materials and Methods.....	16
2.3.1 Equipment Description.....	16

2.3.2	Application of Liquid Manure	18
2.3.3	Measurements.....	19
2.4	Results and Discussion.....	22
2.4.1	Soil Composition	22
2.4.2	Soil Pocket and Roughness.....	23
2.4.3	Manure Dispersion	26
2.4.4	Manure Surface Cover.....	32
2.5	Conclusion.....	33
2.6	Acknowledgement.....	34
2.7	References	34
3	Simulation of Soil Forces of a Rolling Tine Using Discrete Element	
	Method	37
3.1	Abstract.....	37
3.2	Introduction	39
3.2.1	Objectives	43
3.3	Methodology.....	43
3.3.1	Soil-tool Interaction Model	44
3.3.1.1	Soil Particle Model	44
3.3.1.2	Tool Model.....	46
3.3.2	Determination of Model Parameters.....	48
3.3.2.1	Model Particles	48
3.3.2.2	Bond Parameters.....	49
3.3.2.3	Ball Parameters.....	50
3.3.3	Calibration of Ball and Bond Stiffness	51
3.3.4	Model Validation.....	51
3.4	Results and Discussion.....	52
3.4.1	Calibration Results	53
3.4.2	Model Validation.....	55
3.4.3	Model Applications.....	57

3.5	Conclusion.....	59
3.6	Acknowledgements	60
3.7	References	60
4	General Conclusions	63
	Back Matter	64
	References	64

List of Tables

Table 1: Soil Composition	23
Table 2: Summary of the model parameters	53

List of Figures

Figure 1: The rotary tine aerator	3
Figure 2: Field manure application equipment; a) applicator set-up; b) pump; c) manure distribution valve; d) shatter tine and drop tubes.....	18
Figure 3: Soil profiler used to reproduce the shape of the soil disturbances; (a) field measurements (b) processed profile data.....	20
Figure 4: Soil sampling set-up; a) soil probe; b) measurement grids in relation to the soil pocket.....	21
Figure 5: Manure surface cover measurement; a) metal mesh; b) soil surface covered with manure bands	22
Figure 6: Soil disturbance; (a) photo showing soil surface disturbance; 9b) profiles of two transects of a soil pocket illustrating variability in pocket shapes and soil roughness	24
Figure 7: Overthrown soil, pocket size, pocket width, and pocket depth means (with standard error bars) at different tractor speeds	26
Figure 8: Average soil moisture (d.b.) plane from the treatment 42 000 L/ha (4500 gallons/acre) at various depths; (a) 50 mm; (b) 100 mm; (c) 150 mm; (d) 200 mm; (e) 250 mm; (f) 300 mm.....	30
Figure 9: Average soil moisture (d.b.) along the center line from the treatment 42 000 L/ha (4500 gallons/acre) at different depths; (a) forward direction; (b) lateral direction.	31

Figure 10: Means (with standard error bars) of manure surface cover at different tractor speeds.....	33
Figure 11: AerWay shatter tines; (a) mounted on the tractor toolbar; (b) pair of shatter tines penetrating into soil during a field operation	44
Figure 12: Soil model to simulate adhesive silt loam soil in PFC ^{3D}	45
Figure 13: AerWay shatter tine model; a) front view of a tine; b) back view of a tine; c) a rolling tine with four shatter tines; where α is the angular rotation, v is the linear velocity, and r^* is the effective radius of the rolling wheel.....	47
Figure 14: Soil-tool model before simulation.....	48
Figure 15: Virtual soil penetration test using PFC ^{3D}	51
Figure 16: Cone index measurements; a) average cone index from the field; b) simulated cone index to a depth of 200 mm.....	54
Figure 17: Simulated average cone indexes at different ball stiffness (K_n & K_s).....	55
Figure 18: Screenshots of the soil-tool simulation over one shatter tine insertion from a) through d).....	56
Figure 19: Simulated and literature values of draft forces at various working depths with 0° swing angle.....	57
Figure 20: Sample of the simulated vertical force at 150 mm depth	58
Figure 21: Simulated average vertical force of the shatter tine at different working depths at 0° swing angle.....	59

List of Symbols

The following section provides a list of symbols used throughout the paper.

Symbol	Meaning
\bar{K}_n	Bond normal stiffness (Pa/m)
\bar{K}_s	Bond shear stiffness (Pa/m)
\bar{R}_m	Bond radius multiplier
$\bar{\sigma}$	Bond normal strength (Pa)
$\bar{\tau}$	Bond shear strength (Pa)
a	Acceleration of the ball(m/s ²)
c	Soil cohesion (Pa)
F	Corresponding force (N)
k	Ball stiffness (N/m)
K_n	Normal stiffness (N/m)
K_s	Shear stiffness (N/m)
m	Mass of the ball (kg)
r^*	Effective radius of tool rotation (m)
v	Linear velocity of tool (m/s)
x	Ball deformation (m)
α	Angular rotation of tool (rad/s)

ϕ	Internal soil friction angle ($^{\circ}$)
μ	Friction coefficient
BEM	Boundary Element Methods
DEM	Discrete Element Method
FEM	Finite Element Methods
PBM	Parallel Bond Model
PFC ^{3D}	Particle Flow Code in Three Dimensions

Chapter 1

Introduction

The practice of agricultural tillage dates back thousands of years and has dramatically changed over time. As technology and science improve, agricultural practices evolve into a more sophisticated management system, with improved equipment and crop quality. Tillage is defined as the manipulation of soil to provide a suitable medium for plant growth (Georgison 2010). In recent times, there have been two types of tillage that have been commonly practiced known as “conventional tillage” and “conservation tillage”.

Conventional tillage destroys the structure of the soil surface, mixes soil within the ploughed layer and covers the macro-pores within the soil (Andreini and Steenhuis 1990). Soil degradation and intensive energy requirements are often associated with conventional tillage. Conservation tillage is an alternative practice that modifies the soil structure while retaining a minimum of 30% residue cover on the soil surface after planting (ASAE Standards 2004). Conservation tillage has many benefits which include soil protection from erosion, reducing compaction, conserving moisture and reducing energy cost. This alternative practice improves soil structure and stability resulting in better

drainage and water holding capability. The reduced disturbance lowered energy costs and also reduced the amount of carbon dioxide released into the atmosphere (Holland 2004).

The rotary tine aerator is a relatively new tool for conservational tillage and limited soil-tool interaction studies is found in literature sources. The aerator has been developed by various companies (e.g. AerWay, HCC Inc.) for the purpose of penetrating compaction layers while minimizing crop disturbances. Figure 1 shows the rolling tine aerator mounted with the AerWay shatter tines. The aerator uses rotating tines to cleave the soil to a given depth depending on the size of the tine (Georgison 2010). The aerator is designed to have adjustable swing angles between zero and ten degrees relative to the toolbar for the level of tillage aggressiveness. As the angle increases, more of the broad side on the rolling tine is exposed against the soil and displaces more soil along the travel direction.



Figure 1: The rotary tine aerator

Another application of the rotary aerator is to incorporate manure into the soil to maximize the nutrient spread throughout the soil profile. Liquid manure has been applied for agricultural practices as a cost efficient source of nutrients by recycling animal by-products and wastewater generated at the farm. However, misuse of manure applications can cause deterioration of soil quality, volatilization of harmful gases, and can be a source of pollution to water resources (Landry 2005). It is important to optimize the use of nutrient uptake by improving management practices while reducing the environmental impact. Therefore, evaluation of the aerator's performance for manure application is necessary.

The interaction between rolling tines and soil needs to be studied to provide knowledge to optimize future designs and recommendations. Soil-tool interactions have been a continuous challenge for researchers, manufacturers, and users alike. Researchers found that soil and rock materials are difficult to model due to their highly variable properties, non-linear dynamic behaviour, and complex phenomena between the soil, rock and tool surfaces (Shmulevich, 2010). These difficulties have often resulted in many lengthy and costly material behavioural tests to validate soil responses. However, researchers may use tools such as numerical simulations to predict an observation or trend for a given set of parameters without physically replicating a particular scenario. The thesis presents a numerical simulation using the Discrete Element Method (DEM) to model the interactions of soil with the rolling tine.

1.1 General Objectives

The general objectives of the study were to (1) experimentally evaluate the performance (soil disturbance and manure dispersion in soil) of an AerWay shatter tine for liquid manure application, and (2) develop a soil-tool model using DEM for studying the required draft and vertical forces for the shatter tine.

1.2 Application of Modelling Tools

In the past 100 years, knowledge has become increasingly specialized to a point where disciplines started to fragment into different divisions through the advancement of modern research (Nissani 1997). In many cases, one can no longer view problems through a

single disciplinarians' perspective. A single perspective could only illustrate a portion of the complex phenomena that occurs. Therefore, an integrated approach is needed to organize and illustrate the different perspectives on a complex problem. Nicolson et al. (2002) proposed that integrated problems required a bridging of different disciplines when dealing with the complicated interactions that change with both the temporal and spatial scales. In other words, the interactions required knowledge from multiple fields to accurately represent the problem. As a result, one could find and understand the causal effects through a simulation model as opposed to traditional experiments. Nicolson et al. (2002) suggested that simulation models provided a method to unify different disciplines within a coherent frame work and encourage causal relationships defined by the user.

Upon completion of the simulation model, a researcher can explore how the natural problem might respond to different scenarios without going through lengthy experiments to reproduce the same phenomena within a controlled environment. With the rising costs of labour and equipment, many organizations are employing models to predict changes in any system. Despite the many benefits, a simulation model explores only a simplified version of the problem. Researchers should be careful when interpreting the model outputs since simplifying assumptions made within a model may not be valid for all scenarios. Nevertheless, simulation models are an increasingly common tool for researchers to effectively integrate different concepts.

Before creating a model, the researcher is required to organize and consider the many parameters that apply in the virtual model in order to accurately represent a scenario. Star-

field (1997) suggested that a decision making process should be undertaken before a model is created. Starfield (1997) proposed that the model creator must know the objectives of the future work, or the scope of the project. Secondly, it is necessary to have a method of evaluation to determine how well the solution will perform. Commonly, a set of indicators or measurements are needed to compare with simulation outputs. Lastly, the different models and assumptions would be ranked by how well they resemble the situation. Our media of interest is the soil particles interacting with the surrounding materials associated with agricultural practices.

1.3 Understanding the Agricultural Practices

The fundamental parameters of agricultural practices should be understood before researchers can start the modelling process. For agricultural fields, the common goal is to manipulate the soil to optimize crop growth. Tillage of soil and manure application techniques are used to prepare a soil to ensure sufficient oxygen and nutrient levels are available for the crops. Refer to “Chapter 2: Soil Disturbance and Liquid Manure Dispersion in Soil Resulting from a Rolling Tine Liquid Manure Applicator” for an in depth background on manure application.

1.4 Model Evolution

A variety of techniques and assumptions are employed by researchers to simplify the complex interactions within a system. Prior to the availability of computer simulations, mathematicians used a system of simplified mathematical equations to represent a natural

system. One example of a fluid flow simplification is Darcy's law, which measured fluid flow through a particular soil type. This simplification removed the irregularities within the soil material and treated soil as a uniform bulk material (Schwartz 2002). Essentially, the soil lost the microscopic properties such as surface roughness and went from a variable material into a consistent material. Another simplification is Dupuit's equation that treated water flow for unconfined water table as one dimensional flow (Schwartz 2002). An unconfined water table would be present in soils if the geologic formation allowed water to fully saturate the soil above some impermeable layer. The applications of these assumptions are limited and are often considered oversimplifying a complex problem. Despite their ease of application, many mathematical equations often lack the visual representation for others from different disciplines such as a manager or a contractor to comprehend.

With the increasing strength of computer processors, computer simulations are becoming a common tool for many researchers due to the ability to accomplish many computations in a short amount of time compared to traditional experiments. Simulation allowed researchers to deal with more complex problems and interactions without the constraints of many simplifications imposed by many analytical mathematical models. In most cases, behaviours of the natural system are not fully understood, so assumptions or simplifications were required to fill in the gaps. Starfield (1997) mentioned that an incomplete model would still contribute toward a specific research field.

An incomplete model in this circumstance represents the current understanding of a particular system. Despite inaccurate representation of the natural system, the model could still identify useful parameters that illustrate the natural phenomena. The key is to be aware of the assumptions and where there is major disagreement with the observed system. The differences between one's model and the observed measurements act as a validation process to show that the model is relatively similar to the natural problem. Oreskes et al. (1994) mentioned that the justifications of assumptions should also be true for a model to be interpreted in a sensible matter. A common misconception regarding modelling is blindly using modelling as a tool to represent a complex problem without understanding the fundamental concepts.

In practice, there are numerous computer modelling languages that are used to simulate all types of materials. Depending on the discipline area, the preferred programming languages are usually based upon the strengths and weaknesses of representing a particular material. In the past, many geologists and civil engineers have commonly employed Boundary Element Method (BEM), Finite Element Method (FEM) and Discrete Element Method (DEM) as different techniques to assess the ground surface, structures and other materials of interest. BEMs are numerical methods used to solve linear partial differential equations. They can be applied in many areas such as fluid mechanics, acoustics, electromagnetic, and fracture mechanics engineering (Brebbia 1980). FEMs are widely employed as the preferred modelling type for their simplicity and ease of use. FEMs are numerical techniques that allow the material interactions to be connected and act like one object. Applications for FEMs include structural analysis, material testing, and mapping

water resources. Despite FEMs being commonly used for geotechnical problems, soil particles on a microscopic level do not act like one object. Soil particles are often discrete particles that are separable and are not bound together in soil and rock analysis. The overall deformation through FEMs analysis will account for the majority of the total deformation, but some microscopic properties between the soil particles are often lost. Ultimately, this leads to the application of DEMs, which provides a method to apply dynamic behaviours to individual particles and treat each particle as its own entity. To compensate for the added details on a microscopic level, additional processor power is needed to store and compute Newton's law for each particle in every calculation cycle. In the past, DEMs have been used to simulate the flow of many biological materials with the objective of improving the design and performance of material handling machines (Tijssens et al. 2003).

1.5 Model Development

Previous geotechnical and civil engineer developers have identified a list of model parameters to represent the complex interactions and variability of many soil and rock mechanics. Most soil models include the material physical properties, bonds between particles, dynamic responses, and fracture propagation mentioned in "Chapter 3: Simulation of Soil Forces of a Rolling Tine Using Discrete Element Method". The goal was to provide a detailed and realistic model that can be used to predict an observation for any given set of parameters. For validation purposes, all models must be evaluated against experimental data to decide if the models are an acceptable representation.

1.6 The Challenge – Comparison to Reality

The development process has been accelerated by applying the commercial software to real world problems. However, the challenge lies with accounting for different scenarios and variations within the materials of interest. For a model to be reliable, the parameters used, such as particle size, shape, internal friction angle, stiffness, shear and compression strengths, have to be validated experimentally (Coetzee 2009). Aside from calibration of a model's operating parameters, the challenge is to also create a model that is descriptive enough to explain the multiple variations that can occur in a soil sample. The model should be flexible enough to get sufficient value for the time spent on creating a model (Starfield 1997). Coetzee explained that DEM is a very promising approach to model granular material interactions, but the accuracy of the models would depend on the model parameters.

For a model to be influential toward a given field, the model must be validated (Starfield 1997). However, “verification and validation of numerical models of natural systems is impossible” (Oreskes et al. 1994). They explained that natural systems were never a closed model and models were used to demonstrate an agreement between observation and predictions. Since natural phenomena are not completely understood, models can be only evaluated in relative terms and their predicted values have to be used with care due to simplifying assumptions. Even though verification and validation is impossible, models are often useful representations and guides that allow the research to be extended (Oreskes et al. 1994).

1.7 Summary

With the evolution of modern research, modelling is a tool that provides an integrated approach for simplifying a complex problem. The ease and flexibility of numerical simulations have consequently increased the popularity of modelling for research and industry personnel. For soil and geotechnical problems, three common types of numerical simulation are used. They are the Boundary Element Method (BEM), Finite Element Method (FEM) and Discrete Element Method (DEM). Geotechnical and civil engineering developers have identified a list of model parameters that are often used to explain the complex interactions and variability of soil and rock mechanics. They often include material physical properties, bonds between particles, dynamic responses, and fracture propagation. These parameters are aimed to provide a detailed and realistic model that could be used to predict an observation for any given set of parameters. It may be impossible to produce an exact replica of a particular system, but the goals are to fabricate a model that can represent a natural system without too many differences.

Chapter 2

Soil Disturbance and Liquid Manure

Dispersion in Soil Resulting from a

Rolling Tine Liquid Manure Applica-

tor

2.1 Abstract.

The evaluation of manure application techniques for agricultural practices is critical in order to optimize future design and manure application. A liquid manure applicator with AerWay shatter tines and drop tubes were used to study the soil disturbance and the liq-

liquid hog manure distribution following manure application. Liquid hog manure containing 0.4 % total solid content was applied in a silt loam site with barley stubble near Steinbach, Manitoba, Canada in the experiment. Three manure application rates of 23 000, 42 000, and 70 000 L/ha were used, and they were applied at a tractor speed of 0.85, 1.30, and 1.52 m/s, respectively. The field measurements included the soil surface profile, soil samples and the manure surface cover. Effects of the tractor speed and application rate were statistically insignificant to all these variables measured. However, the results indicated the increased tractor speed would increase the soil pocket size and decrease the amount of soil overthrown. Liquid manure dispersion in soil was also measured for the manure application rate of 42 000 L/ha. The results showed that manure dispersed to a maximum depth of 250 mm, while the dispersion spread 200 mm in the forward direction and 100 mm in the lateral direction approximately one hour after the manure application.

Keywords. Liquid manure, dispersion, soil, roughness, pocket, shatter tine

2.2 Introduction

Liquid manure has been applied in agricultural practices as a cost efficient source of nutrients for crop production. The main components of manure are animal feces, urine, wasted feed, water, and soiled bedding. It may also contain material not directly from the livestock excretion such as soil, wastewater, and animal debris (Laguë et al. 2005). Both on farm and off farm manure recycling for crop production are popular since they provide a sustainable nutrient source and water recycling process if managed correctly. As a result, a lower amount of chemical fertilizers and irrigation water are required for crop pro-

duction. The use of liquid manure plays a positive role on microbial activity, and influences the chemical and physical properties of the soil. However, misuse or overuse of manure applications can cause deterioration of soil quality, volatilization of harmful gases, and can become a source of pollution to water resources (Landry 2005). Therefore, it is important to optimize management practices to match manure application to plant nutrient uptake to reduce the environmental impact. Machinery, soil and liquid manure interactions provide knowledge to optimize future designs and recommendations for land application of liquid manure.

Four common techniques are used for liquid manure land application and each has its own set of strengths and weaknesses (Chen et al. 2001). Broadcasting surface application spreads manure on the soil surface over a certain width from a single location (e.g. irrigation gun, single splash plate, rear or side solid manure spreader) or from multiple sources (e.g. irrigation boom, multiple splash plates) (Laguë et al. 2005). Banding surface application uniformly spreads bands of manure from multiple sources such as drop tube systems, and dribble bar systems (Laguë et al. 1994; Oh et al. 2004). Both surface applications use less energy during application, but generate a greater chance for volatilization and manure runoff (Jokela et al. 1996). As a result, more energy consuming methods (e.g. direct injection and incorporation) were introduced to reduce volatilization and runoff opportunities (McLaughlin et al. 2006; Nyord et al. 2008). Direct injection applies manure under the soil surface using some tillage tool (e.g. coulters, disks, and sweeps) or through the use of high pressure injectors (Chen 2002; Chen and Ren 2002; Chen and Tessier 2001; Rahman et al. 2001; Warner et al. 1988). Manure incorporation uses sur-

face application techniques combined with regular tillage operations (e.g. coulters, disks, and rotary tines) to incorporate the manure into the soil profile (Laguë et al. 2005; Rahman and Chen 2001). The main requirement of any land application system is to supply manure that matches the requirements for crop production for any given soil.

Liquid manure incorporated with an aerator maximizes the spread of manure throughout the soil profile. Bittman et al. (2005) and van Vliet et al. (2006) found that manure incorporation with aeration technique offered low crop disturbances and noted a decrease in the ammonia emissions. Aeration by definition means to introduce air into the soil profile. An aerator punched holes (pockets) into the soil surface as the tractor moved through the field, which allowed liquid manure to flow through soil pockets, cracks and channels to infiltrate deep beneath the surface layer (Chen et al. 2001; Harrigan et al. 2004). The shatter tine design used a swing angle and offset to break down compaction layers and recreated the capillary action of the natural soil profile (AerWay 2011), which allowed the much needed nutrients and oxygen to run deep into the plant root zone and spread to areas where they were inaccessible without tillage. The aerator has been considered as an effective tool for liquid manure application due to its advantages of low soil disturbance and power requirement. However, little research has been done to study the soil disturbance and manure dispersion in soil resulting from using an aerator for liquid manure application.

2.2.1 Objectives

In this study, the AerWay commercial shatter tines followed by manure drop tubes were tested in a field. The objective was to determine (1) the soil disturbances created by the AerWay shatter tine and (2) the extent of manure cover on soil surfaces and manure dispersion through the soil.

2.3 Materials and Methods

A field manure applicator with the AerWay commercial shatter tines was used to apply liquid hog manure (containing 0.4 % total solid content) on a silt loam site with barley stubble. The site was located near Steinbach, Manitoba, Canada and the experiment was carried out in July 21 2009. The experiment was a completely randomized design (CRD) with three treatments and four replicates per treatment for a total of 12 plots. Treatments were three manure application rates: 23 000, 42 000, and 70 000 L/ha, which were used as treatments to study how the shatter tines affected the liquid manure dispersion. The three manure application rates corresponded to three tractor travelling speeds of 0.85, 1.30, and 1.52 m/s, which were used as treatments to study how the shatter tines disturbed the soil. The shatter tine was set to a working depth of 150 mm and with a 5° toolbar swing angle.

2.3.1 Equipment Description

The field manure applicator (Figure 2a) consisted of a tractor, manure storage tank, pump (Figure 2b), manure distribution valve (Figure 2c), and a toolbar mounted with AerWay

shatter tines and drop tubes (Figure 2d). The tractor, CaseIH MX120 Maxxum with an 89.5 kW engine, was used to pull the toolbar. Two 170 L tanks filled to about 90% full with liquid manure were mounted onto the toolbar to provide the manure and the weight to ensure the shatter tines penetrated into the soil. A cast iron pump (Figure 2b), Red Lion 5RLGF distributed the liquid manure through four 50.8 mm PVC pipelines to the drop tubes behind the shatter tines. The toolbar mounted four pairs of hubs 400 mm apart and each hub contained four shatter tines for a total of eight hubs and 32 shatter tines on the toolbar. However, only two pairs of hubs were applied with liquid manure.

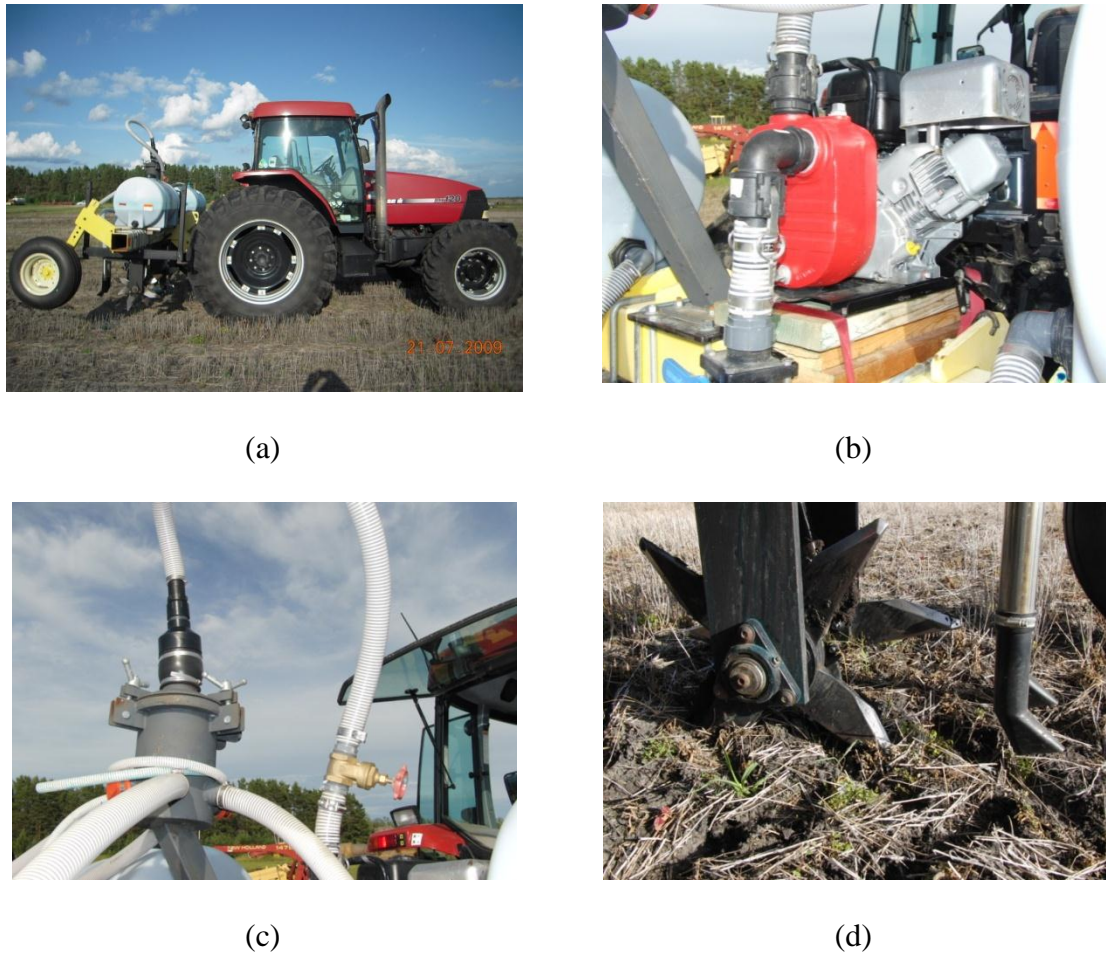


Figure 2: Field manure application equipment; a) applicator set-up; b) pump; c) manure distribution valve; d) shatter tine and drop tubes

2.3.2 Application of Liquid Manure

The manure used in this experiment was from a swine operation secondary lagoon in Southern Manitoba and was found to contain 0.4% total solids by mass. A Brilliant Blue FCF dye (product no. 05601, Warner Jenkinson Co. Inc., St. Louis, MO) was added into the liquid manure to track the dispersion through the soil. The liquid manure application rates were calibrated prior to the experiment by measuring the discharge through the drop tube in a given period of time. The manure flow rate from the tank was kept constant.

The speed of the tractor was then controlled to 1.52, 1.30, 0.85 m/s to obtain the specified application rates. To prevent solids from settling and blocking the inlets of the pump, the liquid manure in the tanks was stirred before the manure application.

2.3.3 Measurements

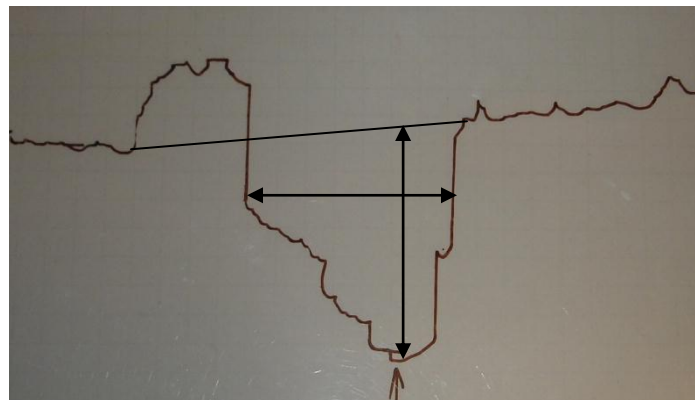
Soil background information: Three soil cores (50 mm diameter, 0-300 mm depth) were taken at random locations of the site. These soil cores were weighed and oven-dried at 105°C for 24 hours to determine the initial soil moisture content (d.b) and dry bulk density. The soil samples were mixed to form a composite sample sent to CanTest Ltd. (Winnipeg, MB, Canada) for soil composition analysis to determine the percentage of sand, silt, and clay, as well as a particle size analysis. The particle analysis followed American Society for Testing and Unified Soil Classification Systems, while the particle size limits were defined in accordance to ASTM (D-2487) classification (ASTM, 2006).

Pocket size & soil roughness: The pocket size and soil roughness were measured using a soil profiler (Tessier et al. 1988). Three soil profiles per plot with four plots per treatment were measured, which resulted in a total of 36 soil profile measurements. This instrument consisted of a number of steel bars that were pushed into the soil to reproduce the shape of the soil profile (Figure 3a). The top outline of the steel bars was traced onto a transparency and the soil profile created by the Aerway aerator was obtained (Figure 3b). The soil profile was characterised using four parameters: the soil overthrown, pocket area, pocket width and pocket depth. The surface topography was estimated by drawing a straight line connecting the exterior ends of the soil profile. The soil profile was placed against 645 mm² graph paper for characterisation. Any amount of soil above the estimated surface

were taken as the soil overturned by the shatter tine, and any void area below were taken to be the pocket size. As for the pocket width and depth, it was measured as the maximum length in the lateral and vertical direction (Figure 3b).



(a)



(b)

Figure 3: Soil profiler used to reproduce the shape of the soil disturbances; (a) field measurements (b) processed profile data

Manure dispersion: The soil samples were taken from the field using a soil probe that was 19 mm in diameter (Figure 4a). The manure was allowed to disperse for one hour in the soil pocket before the soil samples were taken. The soil samples were taken in a grid like fashion and oven dried at 105°C for 24 hours to determine the soil moisture content. The pocket center was positioned at the 100 mm lateral axis and 200 mm forward axis (Figure 4b). Along the forward direction of the tractor, the spacing was 100 mm from 0-

400 mm. As for the lateral direction, the spacing was 50 mm from 0-200 mm and the depth spacing was 50 mm from 0-300 mm. Due to the extensive labour required for this measurement, only one treatment with 42 000 L/ha was measured in three locations from three different plots. In summary, 150 samples were taken from each location for a total of 450 samples. The manure dispersion was evaluated as the difference in moisture content compared to the neighbouring soil conditions (Rahman et al. 2004).

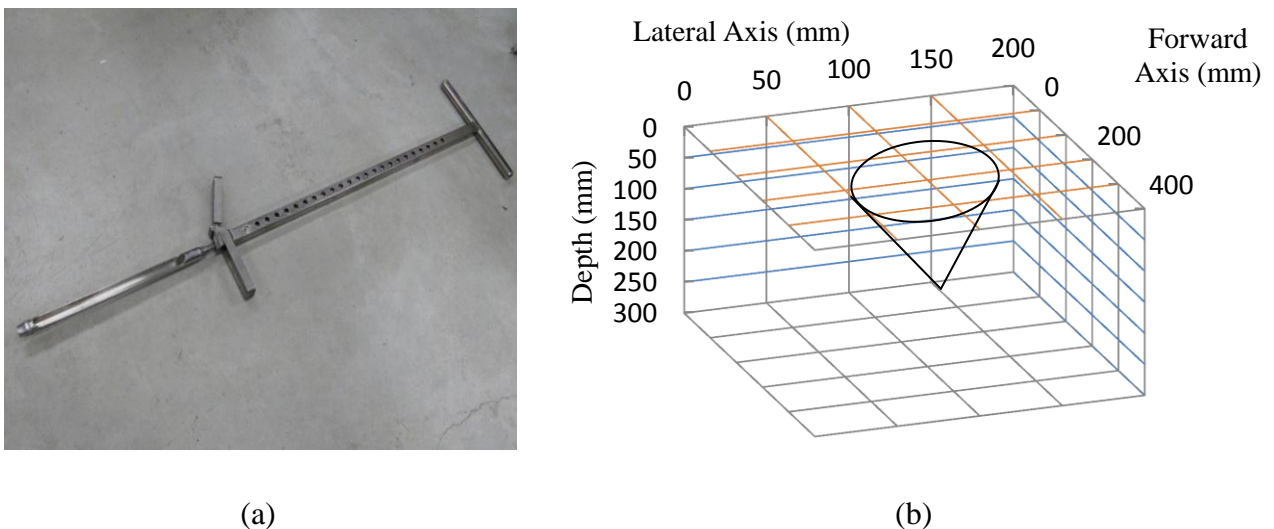
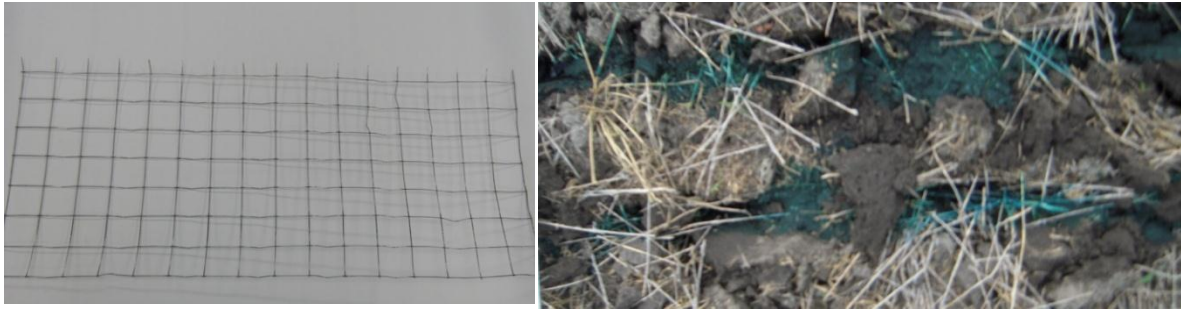


Figure 4: Soil sampling set-up; a) soil probe; b) measurement grids in relation to the soil pocket

Manure surface cover Surface coverage by manure was measured using a metal mesh (400 mm by 800 mm) with 50 mm intervals between nodes (Figure 5a). The metal mesh was placed over the soil surface to cover two manure bands (Figure 5b) to determine the percentage of manure surface coverage. Ten measurements were taken from each plot for a total of 120 measurements. The percentage of manure coverage was determined by the nodes that contained blue dye divided by the total number of nodes on the metal frame and multiplied by 100.



(a)

(b)

Figure 5: Manure surface cover measurement; a) metal mesh; b) soil surface covered with manure bands

2.4 Results and Discussion

2.4.1 Soil Composition

The dry soil bulk density was 0.89 g/cm^3 for the top 150 mm soil and 1.19 g/cm^3 for the lower 150 mm. Similarly, the initial moisture content was found to be 28.1% and 27.4% respectively. From the textural analysis (Table 1), there were two distinct soil layers present at the site. The top 200 mm were classified as a silt loam soil, while 200-300 mm was classified a loam soil (Research branch 1976). As the tillage depth of the rolling tine was 150 mm layer, results from this study are applicable to silt loam soil.

Table 1: Soil Composition

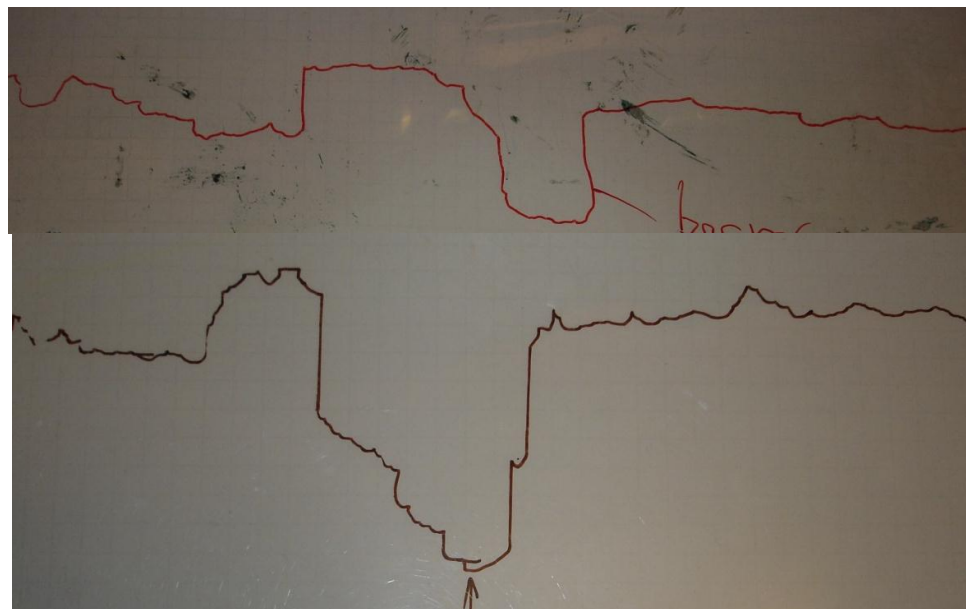
Depth (mm)	% Sand	% Silt	% Clay
0-50	23	53	24
50-100	23	54	23
100-150	24	53	22
150-200	25	57	18
200-250	35	56	10
250-300	42	49	9

2.4.2 Soil Pocket and Roughness

Figure 6a shows the typical soil surface conditions of the field plots. Some barley residue was incorporated into the soil along furrows by the aerator while much of the residue remained on the soil surface between furrows. This demonstrated the low soil disturbance feature of the shatter tines. Many irregular pocket shapes and sizes were measured within the experiment. To illustrate the large range of soil variability, two soil profile measurements are shown in Figure 6b. The parameters of roughness and pocket characteristics were measured from a soil profile which included the amount of soil overthrown, pocket size, pocket width and pocket depth.



(a)



(b)

Figure 6: Soil disturbance; (a) photo showing soil surface disturbance; 9b) profiles of two transects of a soil pocket illustrating variability in pocket shapes and soil roughness

The overthrown soil, pocket size, pocket width, and pocket depth were found to be statistically insignificant between the varying treatments (tractor travel speeds) with an alpha criterion level of 0.05 (Figure 7). Using Scheffe's test, the minimal difference was found to be 9.97 cm², 18.36 cm², 2.64 cm and 2.82 cm for the soil overthrown, pocket size, pocket width, and pocket depth respectively. This resulted in all treatments belonging in the same Scheffe group due to the high standard errors from the measured results. In addition, outliers were present in the data of the soil overthrown with a speed of 1.52 m/s, pocket size with a speed of 1.3 and 1.52 m/s, pocket width with the speed of 0.85 and 1.3 m/s and the pocket depth with the speed of 1.3 and 1.52 m/s based on the externally studentized residual evaluation. The error variances were found to be homogeneous from Bartlett's test and the statistical assumptions were not violated. Although the soil overthrown and pocket size were not significantly different, there was a trend illustrated by the means of each treatment. The data showed that as the speed increased, larger pocket sizes were created and less soil was overthrown. The pocket width and depth were found to have no relationship with the aeration speed. However, the two dimensional snapshots of the soil profile may not fully describe the soil roughness and pocket sizes. To fully describe a soil pocket, multiple transects are required to get a good estimate of the soil pocket parameters.

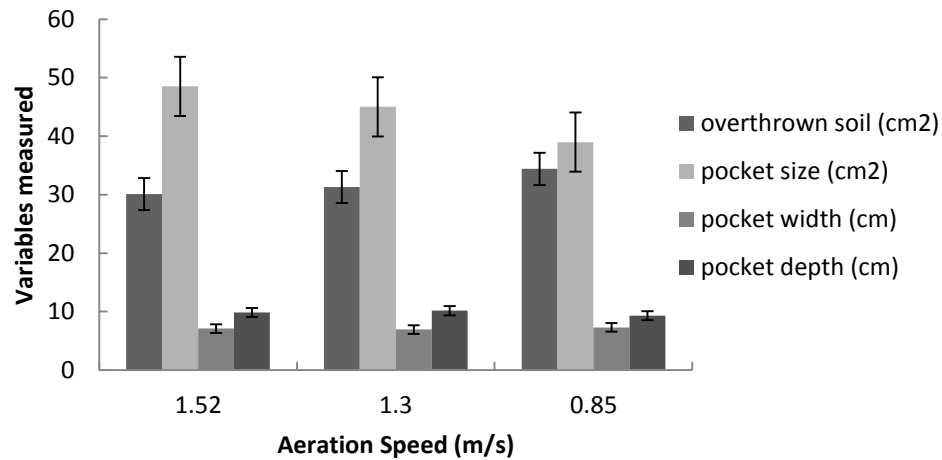
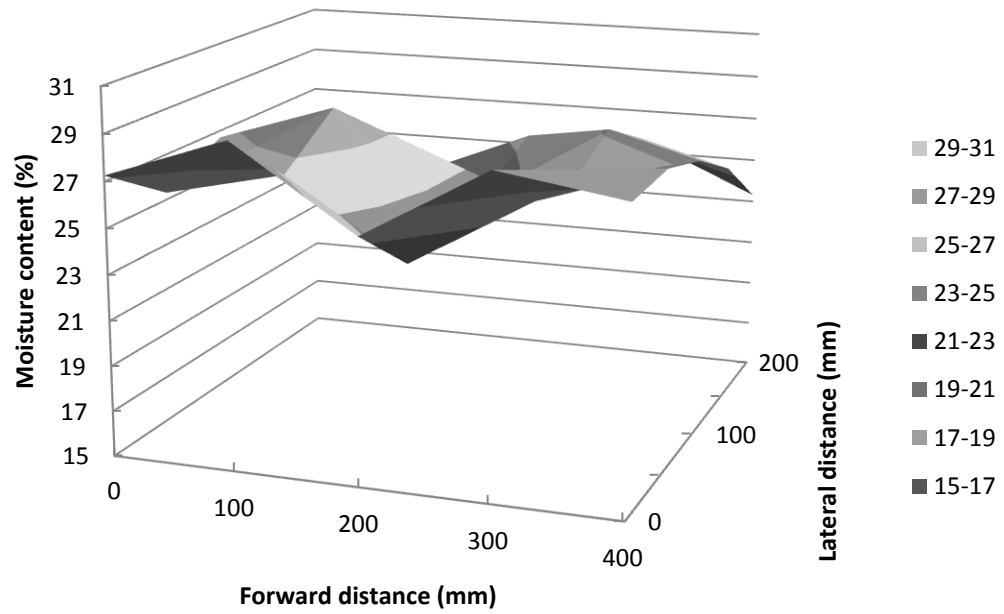


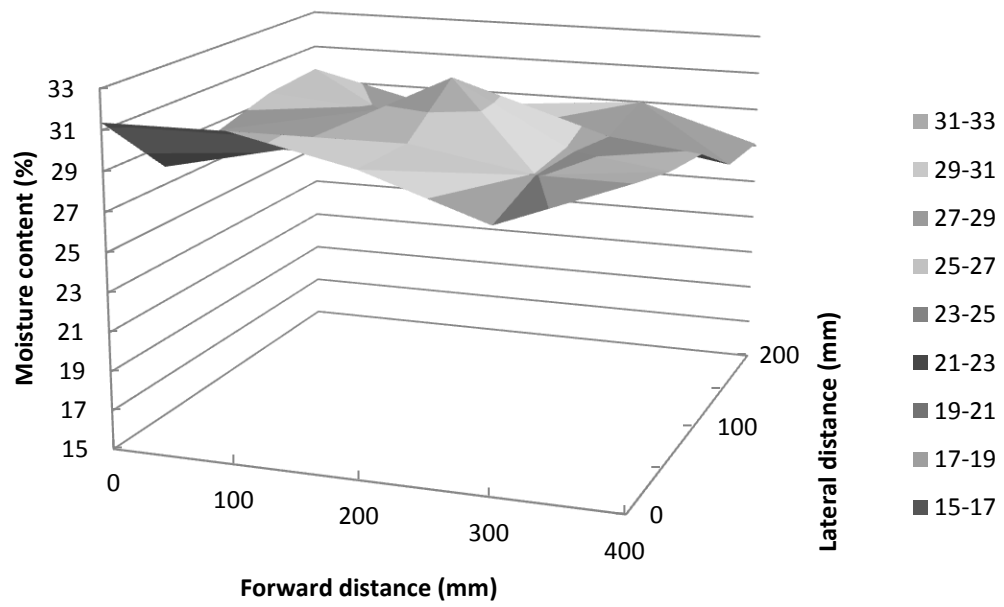
Figure 7: Overthrown soil, pocket size, pocket width, and pocket depth means (with standard error bars) at different tractor speeds

2.4.3 Manure Dispersion

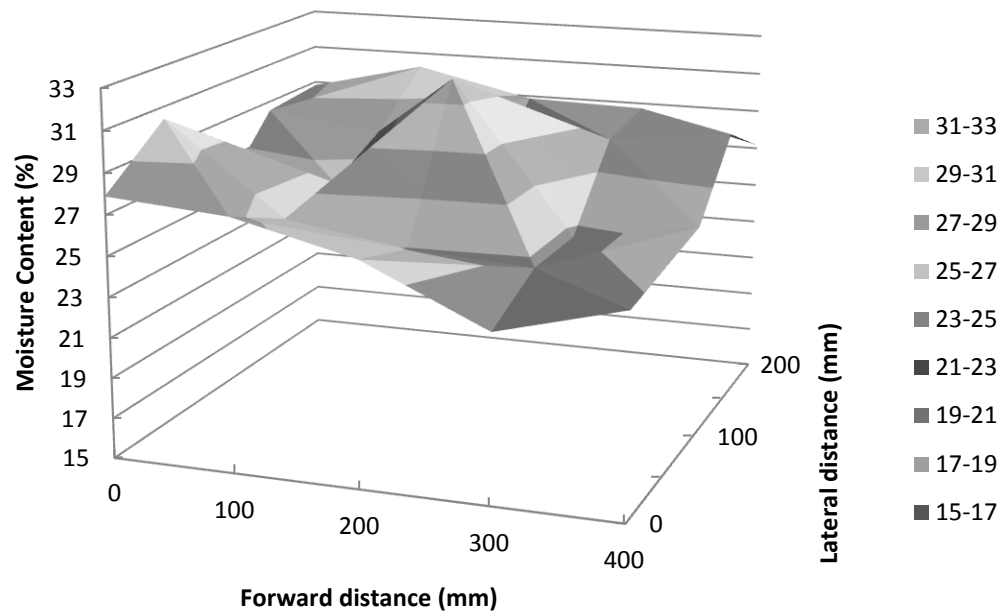
The measurements were shown in a horizontal plane view to illustrate the moisture distribution along the forward and lateral direction resulting from the liquid manure application (Figure 8). Each graph represented the average moisture content at one soil depth. Superimposing all six soil layers gave a 3-D view of how manure dispersed throughout the disturbed soil. The manure application can be seen as the increase of moisture content compared to their surroundings. At the 50 mm depth (Figure 8a), the moisture content was found to be very irregular with the exception of the lower moisture content found between the 100-300 mm in the forward direction. The overthrown dry and loose soil may have fallen back into the soil pocket to influence the moisture readings at the 50 mm depth. Within the 100-300 mm depth (Figure 8b-Figure 8f), there was a clear distinction of the manure concentration found in the middle of the soil pocket in both the forward and lateral direction.



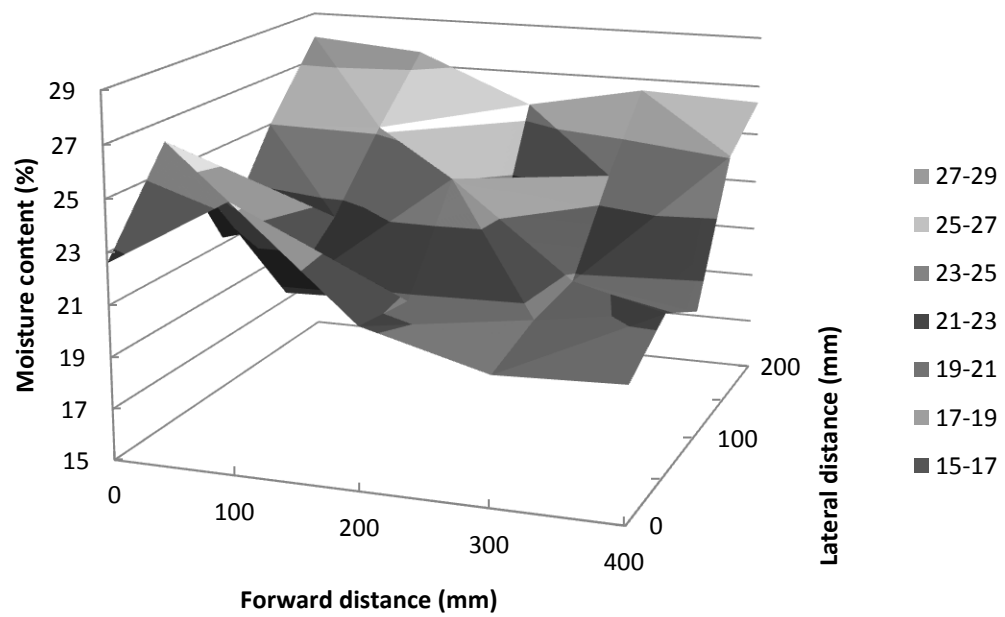
(a)



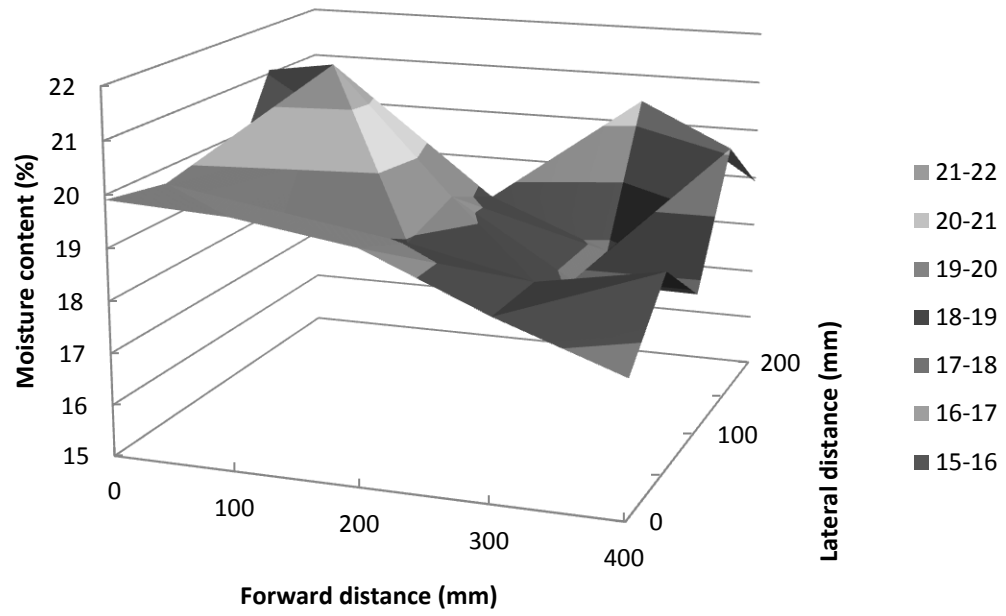
(b)



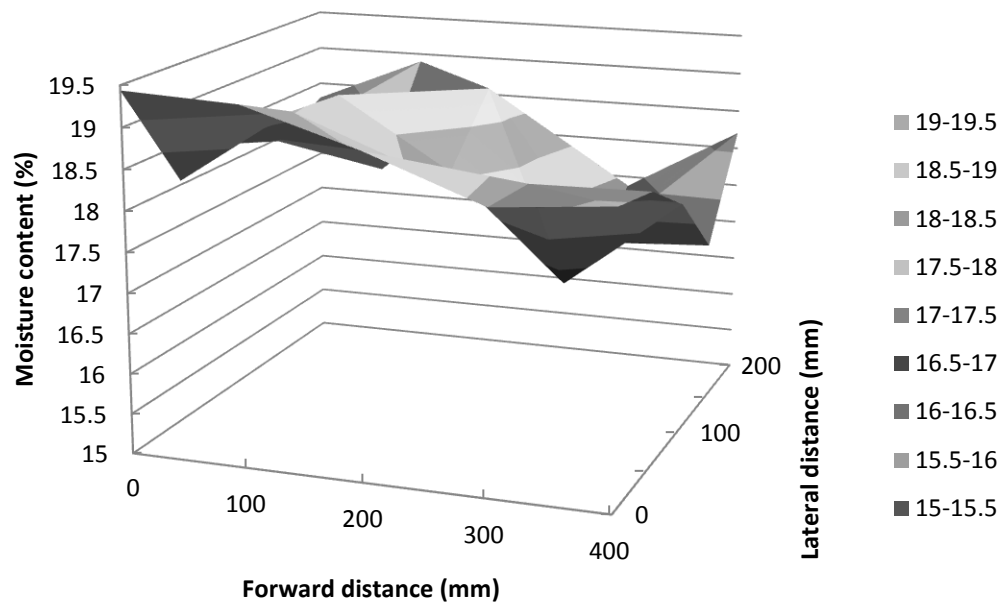
(c)



(d)



(e)

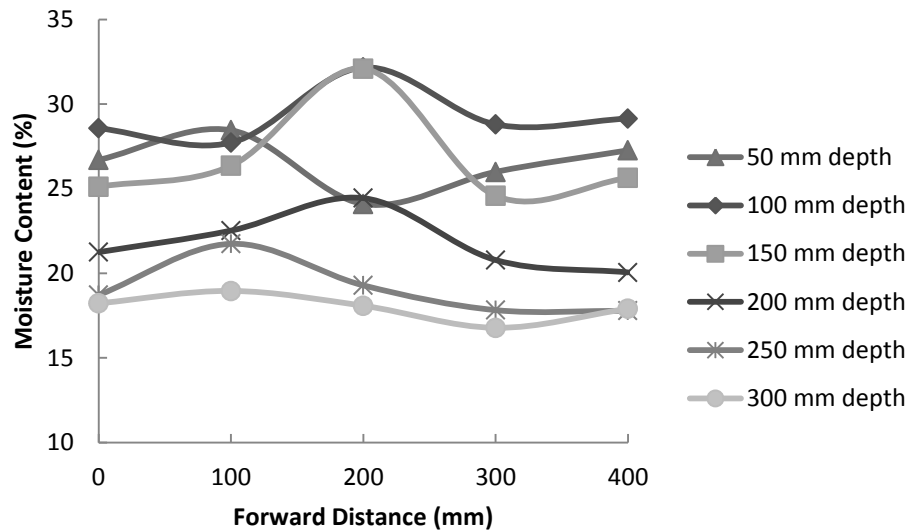


(f)

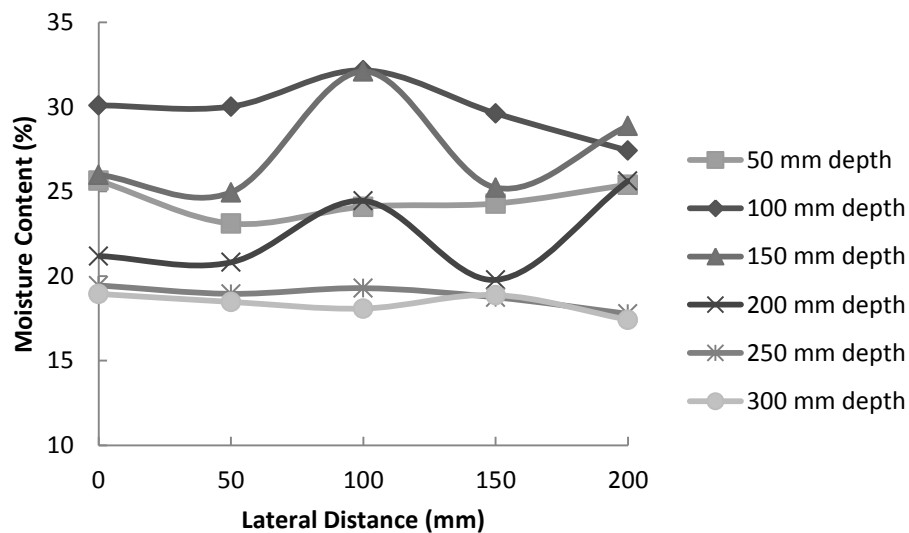
Figure 8: Average soil moisture (d.b.) plane from the treatment 42 000 L/ha (4500 gallons/acre) at various depths; (a) 50 mm; (b) 100 mm; (c) 150 mm; (d) 200 mm; (e) 250 mm; (f) 300 mm

Two additional views were constructed from Figure 8 to further illustrate how the manure application influenced the moisture dispersion within the soil (Figure 9). The center of the soil pocket was located at the 200 mm in the forward distance axis and 100 mm in the lateral distance axis. This curve showed the manure spread along the forward direction was between 100-300 mm from 50-200 mm depth (Figure 9a). However, the spread occurred at the depth of 250 mm was found between 0-200 mm in the forward direction. This would indicate that the tip of the shatter tine may have caused fractures up to 250 mm depth and created a path of preferential flow. Similarly, the spread along the lateral direction occurred between 50-150 mm from 50-200 mm depth and no further dispersion was found below that depth (Figure 9b). The shape of the moisture curve indicated that

the shatter tine created large voids along the center line for liquid manure storage, which reflected the increase of the moisture content within that region.



(a)



(b)

Figure 9: Average soil moisture (d.b.) along the center line from the treatment 42 000 L/ha (4500 gallons/acre) at different depths; (a) forward direction; (b) lateral direction

It was shown that the manure dispersed to a maximum depth of 250 mm depending on the region (Figure 9a). The soil moisture planes (Figure 8) illustrated a clearer picture of

the manure application influence with respect to the surroundings. These measurements indicated that it would be favourable to keep crop spacing to 100 mm in the lateral direction, 200 mm in the forward direction, and maximum root depth of 250 mm to avoid excessive nutrients being inaccessible to root uptake.

2.4.4 Manure Surface Cover

The manure surface cover was found to be statistically insignificant between the varying treatments (manure application rates) with an alpha criterion level of 0.05. The results showed that a relatively constant percentage of the surface (25-30%) was covered by manure and no distinct trends seem to be present with the surface cover (Figure 10). Using Scheffe's test, the minimal difference was found to be 4.03 for the manure surface cover and resulted in all treatments belonging in the same Scheffe group due to the high standard errors. However, outliers were noted for the treatment of 42 000 L/ha from the externally studentized residual evaluation. An explanation for this observation could be the high infiltration rate of the soil and the low total solid content of the liquid manure. The manure was allowed to quickly penetrate vertically through the soil before the manure spread onto the soil surface.

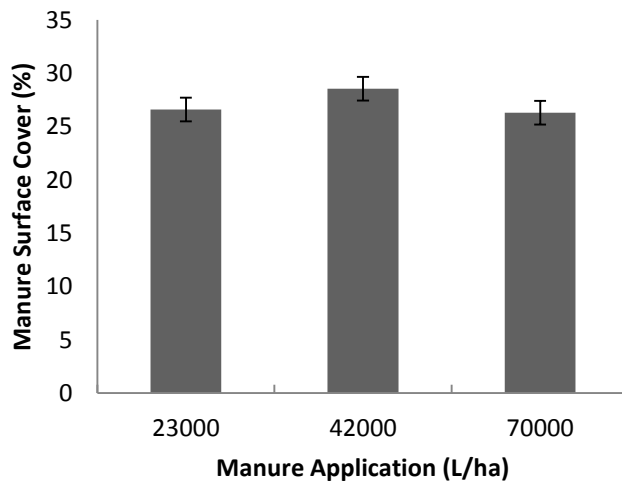


Figure 10: Means (with standard error bars) of manure surface cover at different tractor speeds

2.5 Conclusion

The AerWay shatter tines set to 150 mm depth and 5° offset have shown that the faster tractor speed would create larger pockets and minimize the amount of soil overthrown; however they were not statistically different among the varying speed treatments due to the high variability within each treatment. The pocket width and depth between the varying speeds were found to be statistically insignificant and no particular trends were observed. However, two dimensional soil profiles may not fully describe the soil disturbances caused by the aerator. The liquid manure dispersed to a maximum depth of 250 mm, and the dispersion spread was approximately 200 mm in the forward direction and 100 mm in the lateral direction. Statistically, there were no differences or trends found between the manure application rates on the manure surface cover.

2.6 Acknowledgement

Thanks are given to Mr. Song Ai, Mr. Mohammed Al-Amin Sadek, Mr. Majibur Rahman Khan Mr. Jinke Xu and Mr. Klayton Kaleta, for their help on field work, and to Mr. Scott Dick and Porcherie Gauthier (swine operation) for supplying the manure, and to Dr. Sylvio Tessier for running and setting up the manure applicator.

2.7 References

- AerWay. 2011. The AerWay Difference. Available at: www.aerway.com. Accessed 17 May 2011.
- ASTM Standards. 2006. D-2487: Standard Practice for Classification of Soils for Engineering Purposes (Unified Soil Classification System). ASTM International, West Conshohocken, PA, 2006, DOI: 10.1520/D2487-06E01, www.astm.org.
- Bittman, S., L. J. P. Van Vliet, C. G. Kowelanko, S. McGinn, D. E. Hunt and F. Bounaix. 2005. Surface-banding liquid manure over aeration slots: a new low-disturbance method for reducing ammonia emissions and improving yield of perennial grasses. *Agronomy Journal* 97: 1304-1313.
- Chen, Y. 2002. A Liquid Manure Injection Tool Adapted to Different Soil Conditions. *Transactions of the ASAE* 45(6): 1729-1736.
- Chen, Y. and S. Tessier. 2001. Criterion for Design and Selection of Injection Tools to Minimize Liquid Manure on the Soil Surface. *Transactions of the ASAE* 44(6): 1421-1428.
- Chen, Y. and X. Ren. 2002. High performance tool for liquid manure injection. *Soil and Tillage Research* 67: 75-83.
- Chen, Y., Zhang, Q. and D.S. Petkau. 2001. Evaluation of different techniques for liquid manure application on grassland. *Applied Engineering in Agriculture* 17(4): 489-496.

- Harrigan, T. M., B. B. Bailey, W. J. Northcott, A. N. Kravchenko, and C. A. M. Laboski. 2004. Field Performance of a Low-Disturbance, Rolling Tine, Dribble-Bar Manure Applicator. *Applied Engineering in Agriculture* 22(1): 33-38.
- Jokela, W.E., S.C. Bosworth, P.D. Pfluke, J.J. Rankin and J.E. Carter. 1996. Ammonia volatilization from broadcast and band-applied liquid dairy manure on grass hay. *Agronomy Abstracts*. Madison, Wisconsin: American Society Agronomy.
- Laguë, C., P.-M. Roy, L. Chénard and R. Lagacé. 1994. Wide-span boom for band-spreading of liquid manure. *Applied Engineering in Agriculture* 10(6): 759-763.
- Laguë, C., H. Landry and M. Roberge. 2005. Engineering of land application systems for -livestock manure: A Review. *Canadian Biosystems Engineering* 47: 6.17-6.28.
- Landry, H. 2005. Numerical modeling of machine-product interactions in solid and semi-solid manure handling and land applications. Unpublished Ph.D. thesis Department of Agricultural and Bioresource Engineering, University of Saskatchewan, Saskatoon, SK.
- McLaughlin, N.B., Y.X. Li, S. Bittman, D.R. Lapen, S.D. Burt and B.S. Patterson. 2006. Draft requirements for contrasting liquid manure injection equipment. *Canadian Biosystems Engineering* 48: 2.29-2.37.
- Nyord, T., H.T. Sogaard, M.N. Hansen and L.S. Jensen. 2008. Injection methods to reduce ammonia emission from volatile liquid fertilizers applied to growing crops. *Biosystems Engineering* 100 (2): 235-244.
- Oh, I.H., J. Lee and R. T. Burns. 2004. Development and evaluation of a multi-hose slurry applicator for rice paddy fields. *Applied Engineering in Agriculture* 20(1): 101-106.
- Rahman, S. and Y. Chen. 2001. Laboratory investigation of cutting forces and soil disturbance resulting from different manure incorporation tools in loamy sand soil. *Soil and Tillage Research* 58: 19-29.
- Rahman S., Y. Chen, Q. Zhang, S. Tessier and S. Baidoo. 2001. Performance of a liquid manure injector in a soil bin and on established forages. *Canadian Biosystems Engineering* 43: 2.33-2.40.
- Rahman S., Y. Chen, K. Buckley and W. Akinremi. 2004. Slurry Distribution in Soil as influenced by Slurry Application Micro-rate and Injection Tool Type. *Biosystems Engineering* 89(4): 495-504.
- Research branch. 1976. Glossary of Terms in Soil Science. Canada Department of Agriculture, Ottawa. Publication 1459: 44.

- Tessier, S., Saxton, K.E., Papendick, R.I., and G.M. Hyde. 1988. Measurement of the physical properties of the soil-seed environment. CSAE Paper No. 88-215. Calgary, Alberta.: CSAE.
- Van Vliet, L. J. P., S. Bittman, G. Derksen and C. G. Kowalenko. 2006. Aerating Grassland before Manure Application Reduces Runoff Nutrient Loads in a High Rainfall Environment. *Journal of Environmental Quality* 35: 903-911.
- Warner, N.L. and R.J. Goodwin. 1988. An experimental investigation into factors influencing the soil injection of sewage sludge. *Journal of Agricultural Engineering Research* 39(4): 287-300.

Chapter 3

Simulation of Soil Forces of a Rolling Tine Using Discrete Element Method

3.1 Abstract

Soil interaction with a rolling tine (AerWay shatter tine) was modeled using a commercial software called PFC^{3D} (Particle Flow Code in Three Dimensions) based on the Discrete Element Method (DEM). The model parameters were calibrated using soil cone index field data from a silt loam soil. The calibrated model particles had the particle stiffness (k_n and k_s) of 10 kN/m and bond stiffness (\overline{K}_n and \overline{K}_s) of 1 kPa/m. The model can predict the required draft forces to pull the shatter tine at various depths. The simulated draft forces were compared to literature data and had a relative error of 13.4-31.2% within the 100-150 mm depth. The model can also be used to predict the vertical force of the

shatter tine. The predicted draft force linearly increases with working depth until 150 mm around 700 N per shatter tine and plateau until the full insertion of 200 mm.

Keywords: Discrete element method, PFC^{3D}, Tine, Soil, Force, Depth

3.2 Introduction

Modeling of soil-tool interactions has been a continuous challenge for researchers, manufacturers, and users alike. Researchers have found that soil and rock materials are difficult to model due to their highly variable properties, nonlinear dynamic behaviour, and complex phenomena between the material and tool surfaces (Shmulevich 2010). These difficulties have often resulted in many lengthy and costly material behavioural tests to validate soil responses. However, researchers may use tools such as numerical simulations to predict an observation or trend for a given set of parameters without physically replicating a particular scenario. This paper presents a numerical simulation using the Discrete Element Method (DEM) to model soil-tool interactions in the operation of the AerWay shatter tines.

In 1979, DEM was first introduced by Cundall and Strack (1979) in the field of rock mechanics and is now applied to many disciplines such as modelling the aquifer properties (Burlingame 2008), flow of grain in a silo (Lu et al. 1997), solid manure application (Landry et al. 2006), and soil behaviours (Lim and McDowell 2008). DEM has evolved into a commercial software package known as Particle Flow Code in Three Dimensions (PFC^{3D}) (Itasca Consulting Group Inc., Minneapolis, USA). PFC is a discontinuum code used for simulation of many discrete objects. A basic PFC^{3D} model consisted of spherical balls that simulate the soil particles enclosed within a series of walls which act as the physical boundaries within a specified domain. The desired material properties can be modelled by varying the balls' micro-properties, such as their sizes, number of balls, and

their stiffness. The software uses an iterative approach and with each calculation time step, each ball can contact neighbouring balls or walls, and the dynamics of the assembly is governed by the Newton's laws of motion (Cundall and Strack 1979). Currently, researchers are using particle properties, bonds between particles, dynamic responses, and fracture propagation as comparison criteria to physical materials.

The foundations of most DEM models involve studies on the material properties, such as particle size, particle shape, modulus of elasticity, bond types, bond strengths and particle orientation. Bagherzadeh-Khalkhali and Mirghasemi (2009) studied the influence of particle size on the shear strength of coarse soils and concluded that the particle size and internal friction angle greatly affected the soil behaviour. Similarly, Sakakibara et al. (2008) studied the effects of grain shape, size and material properties that influence the mechanical and shear behaviour of granular materials. Sakakibara et al. (2008) compared different clusters by changing the overlap of three balls to create a series of particle types. They found a linear relationship between the internal friction angles and the defined shape factors. The grain shape was found to affect the respective shear band when the samples were in compression. Lu and McDowell (2007) have also done a similar test in PFC^{3D} with a cluster of spheres to model the material properties of railway ballast under stress. They found that the clusters interlocked and reduced both the displacement and rotation of the particles. Lu and McDowell observed that a three dimensional model created a different spatial parameter that a two dimensional model could not illustrate. Shamy and Gröger (2008) investigated the micromechanical aspect of shear strength on wet granular soils. Their focus was to model the capillary attractive forces present in unsatu-

rated soils. The water tension between the soil particles acted as a bond that kept the particles together until a force could overcome the water tension. They found that the capillary forces and the hydraulic hysteresis played a role in determining the cohesion and stiffness of the soil. Lim and McDowell (2008) measured the void collapse of granular materials and observed that frictionless materials created a change in volume equal to the void collapse. However, frictional material arched to stabilize un-collapsed pore spaces which reduced the consolidation of the soil. The dynamic reaction of a material can greatly impact the output of a model simulation.

Another research area is the fracture variability in soil and rock formations. Potyondy and Hazzard (2008) compared a bonded particle model with laboratory observations containing sandstone to provide a quantitative link between damage development in the bonded particle model and damage development in actual rock. The overall stiffness was reduced 41% during the fracturing phase and the stiffness was reduced an additional 5% after the fractured phase. They also noted that majority of the stiffness change resulted from change of contact points rather than the creation of new cracks. Momozu et al. (2003) compared soil behaviour and energy absorption between the numerical simulation and experimental observation of a blade cutting through soil. Their comparison criteria included two dimensional soil profiles and the total consumed potential energy used to cut through the soil. They concluded that their modified contact model can be extended for explaining the dynamic behaviour of soils. These parameters are aimed to provide a detailed and realistic model that could be used to predict an observation for any given set of parameters. However, it is currently impossible to produce an exact replica of a particular

system; therefore, the goal is to focus on a particular area without compromising the nature of the system (Starfield 1997).

There have been few studies on modeling soil-tool interactions using DEM. Most existing DEM soil-tool models were in 2D and for cohesion-less soils. Franco et al. (2007) modelled soil-bulldozer interaction and van der Linde (2007) modelled soil interaction with a powered subsoiler. In soil-tool interaction modelling using DEM, calibrations of model parameters (such as particle stiffness and particle bond strength) are crucial, as model parameters significantly affect the model outputs. Van der Linde (2007) used compression and direct shear tests to calibrate model parameters for a sandy soil. Asaf et al. (2007) calibrated model parameters based on field sinkage tests for cohesion-less material. Through reviewing DEM modelling of soil-machine interaction, Shmulevich et al. (2009) concluded that there have been no robust methods to determine DEM model parameters.

Rolling tines have been used in agriculture to loosen and aerate soil for better crop growth. Rolling tines have been also used for liquid manure incorporation. Applying liquid manure on aerated soil enhances manure infiltration into the soil. However, little research has been done to study the interaction of rolling tines with soil, and no DEM models have been developed in this regard. In this study, a commercial rolling tine mounted with AerWay shatter tines, was simulated using DEM to observe the dynamic responses of the shatter tine in soil.

3.2.1 Objectives

The objectives of this study were to (1) develop a model using PFC^{3D} to simulate the soil interaction with the AerWay shatter tine, (2) calibrate the model with field data and (3) validate the draft forces of the shatter tine and (4) predict the vertical forces of the shatter tine.

3.3 Methodology

An AerWay commercial shatter tine was used to model the soil-tool interaction during a field operation with the focus on soil forces of the shatter tine. The shatter tine (Figure 11a) can work at a depth from 50 to 200 mm, with a swing angle from 0 to 10°. The aerator consisted of the AerWay roller hubs with four shatter tines mounted 90° from each other. As the tractor moves forward, the shatter tine rotates and punches holes into the soil (Figure 11b). A PFC^{3D} model was developed in this study to simulate the interaction of the shatter tine with soil during its operation. Model parameters were calibrated using field measurements of soil cone index. The field soil was a silt loam (28.7% sand, 53.7% silt, and 17.6% clay) with barley straw stubble and contained 28% moisture content (d.b) in Steinbach, Manitoba, Canada. Cone index was measured using a recording Rimik cone penetrometer (Model CP20, Toowoomba, Australia) with a 30° circular stainless steel cone with 12.83 mm diameter. A total of 27 readings were obtained from nine different locations on the field with three readings per location. The penetrometer recorded the cone index from 0-300 mm at 25 mm increments, while the cone penetrometer was pushed into the soil at a speed of 30 mm/s (ASABE Standards 2006). The model calibra-

tion was to find model parameters that mirrored the soil behaviour by comparing the model results with the field cone index measurements. The soil-tool interaction model was used to predict draft forces of the shatter tines which were validated with literature data.



Figure 11: AerWay shatter tines; (a) mounted on the tractor toolbar; (b) pair of shatter tines penetrating into soil during a field operation

3.3.1 Soil-tool Interaction Model

3.3.1.1 Soil Particle Model

A basic PFC^{3D} model consisted of spherical balls that simulate material particles, such as soil particles, and walls which act as the physical boundaries within a specified domain. Walls can also be used to construct rigid tools such as cone penetrometers and rolling tines. With each calculation time step, each ball can contact neighbouring balls or walls to determine the dynamics of the particle assembly according to Newton's laws of motion (Cundall & Strack 1979). During each time step a force body diagram can be constructed

on each ball to determine the resultant force and direction based on nearby contacts (Equation 1). When the balls come into contact with neighbouring entities, the deformation on each ball is based on the force displacement law (Equation 2). The desired soil properties can be modelled by varying the ball and inter-ball bond properties.

$$F = ma \quad (1)$$

$$F = kx \quad (2)$$

where F is the corresponding force (N), m is the mass (kg), a is the acceleration (m/s^2), k is the stiffness property (N/m), and x is the ball deformation (m).

Several contact models are present in PFC^{3D} to describe the nature of contacts between particles. Typical model types include the stiffness, slip, contact bond, parallel bond and the dashpot models (Itasca 2008). To simulate the cohesive nature of the silt loam soil, the model used parallel bond model (PBM), plus contact bonds and viscous damping between each contact point (Figure 12). The PBM can be envisioned as a cementitious material having a cylindrical shape being installed between particles. These conditions mimic the cohesion of soil, for example, the water film surrounding soil particles that allows the soil particles to be bonded together (Shamy and Gröger 2008).

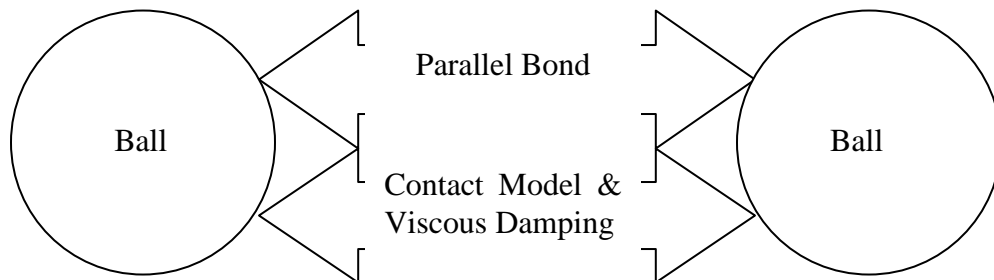


Figure 12: Soil model to simulate adhesive silt loam soil in PFC^{3D}

This model type has eight model parameters, including three ball properties and five bond properties. The ball parameters are normal stiffness: K_n (N/m), shear stiffness: K_s (N/m), and friction coefficient: μ . The bond parameters are normal stiffness: \overline{K}_n (Pa/m), shear stiffness: \overline{K}_s (Pa/m), normal strength: $\overline{\sigma}$ (Pa), shear strength: $\overline{\tau}$ (Pa), and radius multiplier of the cylinder bond: \overline{R}_m (dimensionless). The normal and shear stiffness controls the respective deformation of the ball and bonds that are in contact. The normal and shear strength only applies to the bond's strength between two contacting objects. The bond radius multiplier is the ratio of the cylindrical bond radius between particles and the radius of the smaller ball in contact.

3.3.1.2 Tool Model

The basic tool geometric parameters used in this model were developed to closely match the dimensions of a rolling tine with four AerWay shatter tines. The model tool (Figure 13) has been slightly modified to reduce simulation time by simplifying curved surfaces. The key features of AerWay's design, including the tine length of 201.7 mm, the twist angle of 8° , lean angle of 2.5° , and the bevel angle of 36° were maintained. The basic controllable parameters during tillage operations include swing angle, working depth, and travel speed.

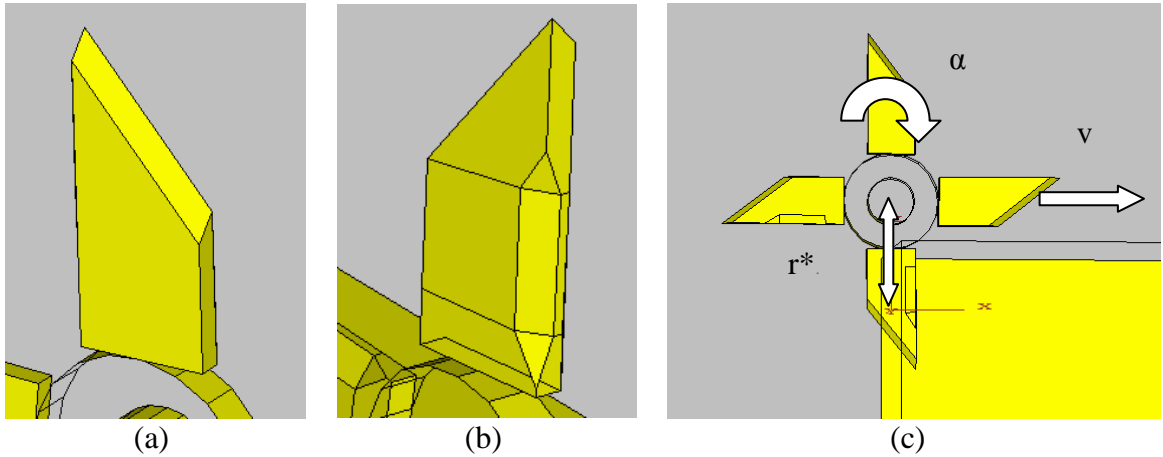


Figure 13: AerWay shatter tine model; a) front view of a tine; b) back view of a tine; c) a rolling tine with four shatter tines; where α is the angular rotation, v is the linear velocity, and r^* is the effective radius of the rolling wheel.

The shatter tine model was constructed with a series of walls using the PFC^{3D} FISH functions. Thirteen walls were generated to construct the shape of the shatter tine and maintained the twist, lean, and bevel angle. A total of 54 walls were used to mirror an AerWay rolling tine consisting of four shatter tines mounted 90 degrees from each other on hubs. Two cylinders were used to create the surface for the shaft and the bearing. The angular rotation of the rolling tine in the model was calculated using Equation 3.

$$\alpha = \frac{v}{r^*} \quad (3)$$

where α is the angular rotation (radians per second), v is the travel velocity, and r^* is the effective radius of the shatter tine.

For the soil-tool interaction model, a finite soil domain was constructed for simulation and validation purposes. The dimensions were chosen to be 400 mm x 2000 mm x 400 mm (width, length, depth) based on the spacing of the shatter tines, depth of interest, and computing power. The model volume was large enough for the modelled tool to cut

through the soil with minimal effects from the wall boundaries. Five walls were used to construct the soil domain to contain the soil particle assembly. The soil assembly used PFC^{3D} FISH functions to fill the soil domain and settled using gravity. The tool was placed at the origin set to a desired depth prior to initiating the simulation of tool operations. The soil-tool model is shown in Figure 14. The black lines represent the contact forces between the soil particles due to gravity.

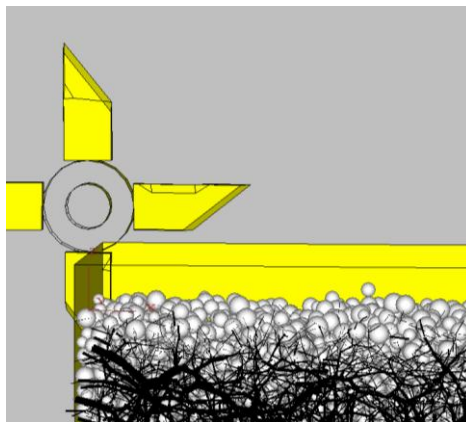


Figure 14: Soil-tool model before simulation

3.3.2 Determination of Model Parameters

3.3.2.1 Model Particles

Model properties are known to have a large impact on outputs of the model. The model particle properties should be calibrated to ensure that the model particles represent the soil. The ball size in the simulation was chosen to follow a random uniform distribution between 10-20 mm due to computing times during simulations. The individual ball sizes were not a huge concern since the PBM allows balls to be bonded and can move together to mirror the movement of larger soil “aggregates”. However, the sizes of the balls should reflect sizes of soil aggregates. Okunlola and Pyne (1991) reported that a range of aggre-

gate size between 1-49 mm worked for both a fine and coarse soil. The average bulk density of 1325 kg/m^3 and a particle density of 2650 kg/m^3 were used to derive the porosity (0.5) of the particle assembly (Campbell 1985).

3.3.2.2 Bond Parameters

The model's parameters cannot be calibrated all at the same time; consequently some parameters were taken from existing studies. To determine bond parameters, soil behaviours were related to PFC^{3D} bond parameters. Water bonds between particles affected the strength of the unsaturated soil by resisting both the shear and tensile loads and often termed as intrinsic stress (Upadhyaya et al. 1994). In the PBM, bonds between particles carry loads, and thus, the bond strengths could be the soil intrinsic stress and cohesion. Therefore, the following equations for soil intrinsic stress and cohesion (McKyes 1985) were used to determine the bond normal and shear strength.

$$\bar{\sigma} = c \cot\phi \quad (4)$$

$$\bar{\tau} = c \quad (5)$$

where $\bar{\sigma}$ is bond normal strength (Pa); c is soil cohesion (Pa); ϕ is internal soil friction angle; $\bar{\tau}$ is bond shear strength (Pa). Soil cohesion and internal soil friction angle can be measured by standard shear tests, but they were taken from literature for a silt soil (Upadhyaya et al. 1994). The cohesion was found to be 2000 Pa and the internal friction angle was 28° . According to Equations (4) and (5), the bond normal stress was found to be 3761 Pa and the bond shear strength was 2000 Pa.

The other bond parameters included the normal stiffness, shear stiffness and the bond radius multiplier. Due to the difficulties of calibrating many parameters at once, Potyondy and Cundall (2004) suggested making logical assumptions for some parameters while other parameters are being calibrated. A bond stiffness ratio ($\overline{K_n}/\overline{K_s}$) of 1 was selected from the range of 1 to 1.5 from a study conducted by Cundall and Strack (1979) for elastic bodies in contact with elliptical contact areas. The bond radius multiplier ($\overline{R_m}$) was chosen as 0.5. Potyondy and Cundall (2004) suggested that when $\overline{R_m} = 0$, the material behaviour approached a cohesion-less material, such as sand and when $\overline{R_m} = 1$, the material behaviour that approached a solid material, such as rock. Another study from van der Linde (2007) has also used the same assumption of $\overline{K_n}/\overline{K_s} = 1$ and $\overline{R_m} = 0.5$.

3.3.2.3 Ball Parameters

The three ball parameters included the normal stiffness (K_n), shear stiffness (K_s) and the friction coefficient (μ). These parameters were not measurable with the current soil dynamic knowledge and needed to be calibrated. To simplify the model, the normal (K_n) and shear stiffness (K_s) were set the same (Asaf et al. 2007; van der Linde 2007). The ball friction coefficient (μ) was given an assumed value of 0.5, which only slightly affected the draft forces of the tillage tool (van der Linde 2007).

At this point, six out of eight model parameters have been determined or assumed. The remaining two parameters, ball and bond stiffness, were calibrated simultaneously using experimental measurements, as discussed in the following sections.

3.3.3 Calibration of Ball and Bond Stiffness

Virtual penetration tests were performed on the soil assembly to simulate soil cone penetration tests. The virtual penetrometer consisted of two walls, one cylinder and one cone (Figure 15). The geometric dimensions of the virtual penetrometer and the insertion speed were set the same as the field cone penetrometer tests. The domain of the soil for the virtual penetration test was reduced to 400 x 400 x 400 mm (width, length, height) to reduce the computation time. Figure 18 shows the virtual penetrometer and the model particles. The black lines represent the contact forces between the soil particles due to gravity.

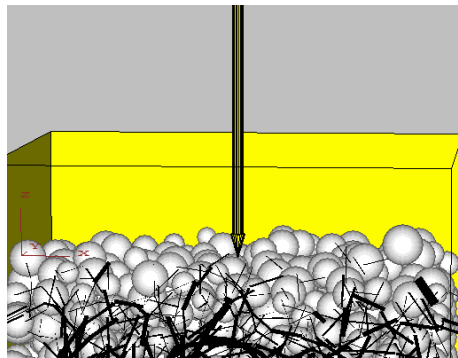


Figure 15: Virtual soil penetration test using PFC^{3D}

3.3.4 Model Validation

The soil-tool interaction model was validated using literature data from McLaughlin et al. (2006). McLaughlin et al. (2006) measured draft forces of the AerWay shatter tines at different depths (75 mm - 150 mm) and swing angles (0, 2.5, 5.0, 7.5, and 10°) in loam soils with barley stubble and clay-loam soils with soybean stubble. Using the data, they

developed a regression equation in which draft force of the shatter tine was a function of working depth at each swing angle as follows:

$$D = cT^2 \quad (6)$$

where D is the draft per meter width (N/m); c is the regression coefficient; T is the working depth (mm). Draft forces predicted from Equation (6) were measured in Newton per meter of the toolbar; they were converted to Newton per rolling hub using the given spacing of the rolling tine. Draft forces simulated by the soil-tool model were validated against the above equation for the 0° swing angle and clay loam soil, which was similar to the soil type used in this study for the model calibration. The modelled draft forces were matched with those predicted from Equation 6 at working depths from 75 -150 mm.

3.4 Results and Discussion

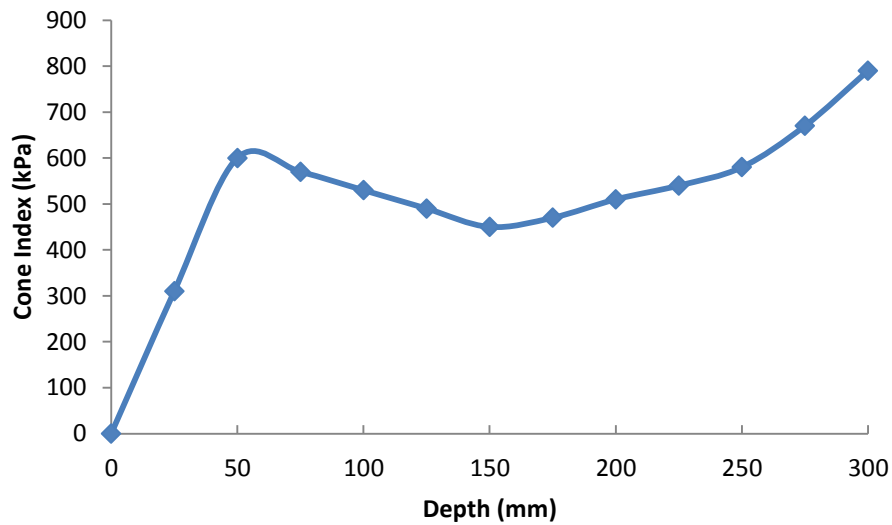
The simulated model randomly generated balls within the soil domain and settled with gravity at 9.81 m/s^2 . A global viscous damping coefficient of 1 was used to damp the particle flight paths. Itasca (2008) suggested that when the damping coefficient is at 1.0, the system is said to be critically damped and the responses decay at the fastest rate to zero. The steel friction coefficient (μ) was found to be 0.42, while the normal (K_n) and shear stiffness (K_s) was found to be $1 \times 10^9 \text{ N/m}$ (Shen and Kushwaha 1998; Godwin 2007). Another study conducted by van der Linde (2007) used similar tool parameters. Due to the limitation of the domain length, a maximum tool working speed of approximately 0.4 m/s was used to ensure stable readings. The values of the tool, ball and bond parameters used in the simulation are summarized in Table 2.

Table 2. Summary of the model parameters

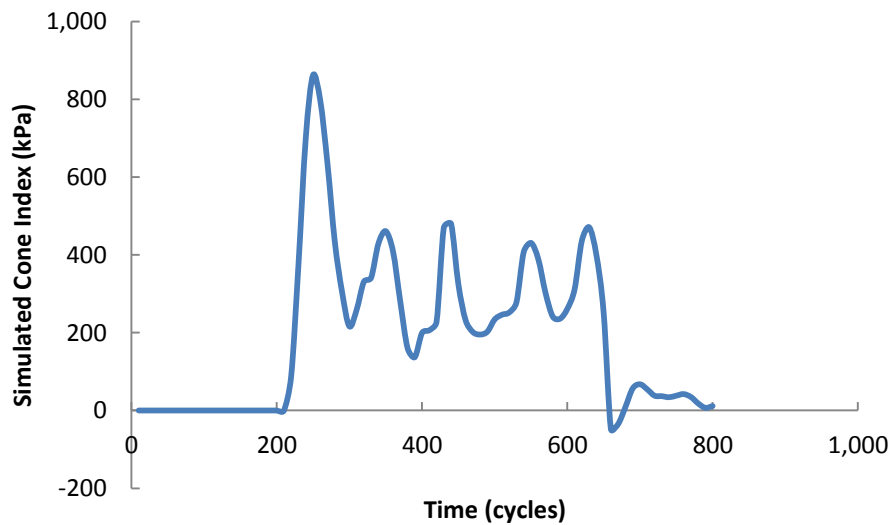
Parameter and symbol	Description and unit	Value
Ball parameter		
μ	Ball friction coefficient	0.5
K_n and K_s	Ball normal and shear stiffness (N/m)	Calibrated Results
K_n/K_s	Particle stiffness ratio	1
Bond parameter		
\overline{R}_m	Radius multiplier	0.5
$\overline{\tau}$	Bond shear strength (Pa)	2000
$\overline{\sigma}$	Bond normal strength (Pa)	3700
\overline{K}_n	Bond normal and shear stiffness (Pa/m)	Calibrated Results
$\overline{K}_n/\overline{K}_s$	Bond stiffness ratio	1
Tool parameter		
μ	Friction coefficient	0.42
K_n and K_s	Normal and shear stiffness (N/m)	1×10^9

3.4.1 Calibration Results

Field soil cone indices were averaged at each soil depth over all locations, and the results are shown in Figure 16a. For model calibration, only the data from 0-200 mm depth were of interest, and the data for this depth range varied from 450 to 600 kPa, which was quite uniform, considering the heterogeneous nature of soil. The model calibration was matched to the average soil cone index of 490 kPa. The simulated cone index fluctuated over time due to the dislocating ball contacts (Figure 16b). Forces simulated with DEM have fluctuating nature (Shmulevich et al. 2009).



(a)



(b)

Figure 16: Cone index measurements; a) average cone index from the field; b) simulated cone index to a depth of 200 mm

To compare with the average field cone index, a series of ball and bond stiffness were simulated and averaged over 200 mm soil depth. It was found that the ball stiffness of 10 kN/m and bond stiffness of 1 kPa/m matched the field measurement the best. The simulated cone index has a relative error of 7.7% when compared to the field measurement. In

the calibration process, it was observed that the simulated cone index was more sensitive to the ball stiffness than to the bond stiffness. Figure 17 demonstrates that the average cone index simulated rapidly increases with the increase in the ball stiffness.

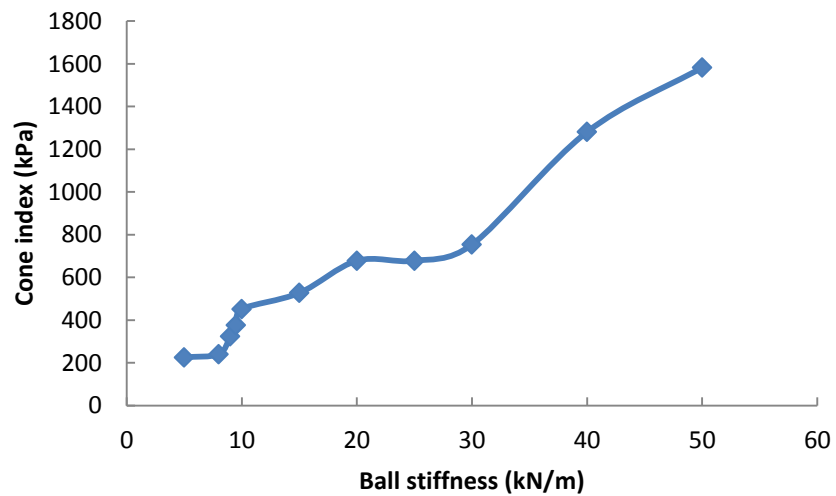


Figure 17: Simulated average cone indexes at different ball stiffness (K_n & K_s)

3.4.2 Model Validation

The soil-tool interaction model was used to simulate the draft forces of the shatter tine. The calibrated ball stiffness of 10 kN/m and bond stiffness of 1 kPa/m were imported into the model. The simulation started at the desired working depth and rotated into the soil medium shown in Figure 18a through Figure 18d. Interestingly, one could study the flight path of the dislodged particles and the force/stress concentration shown as the black lines within the soil domain. However, these topics were outside the scope of this study.

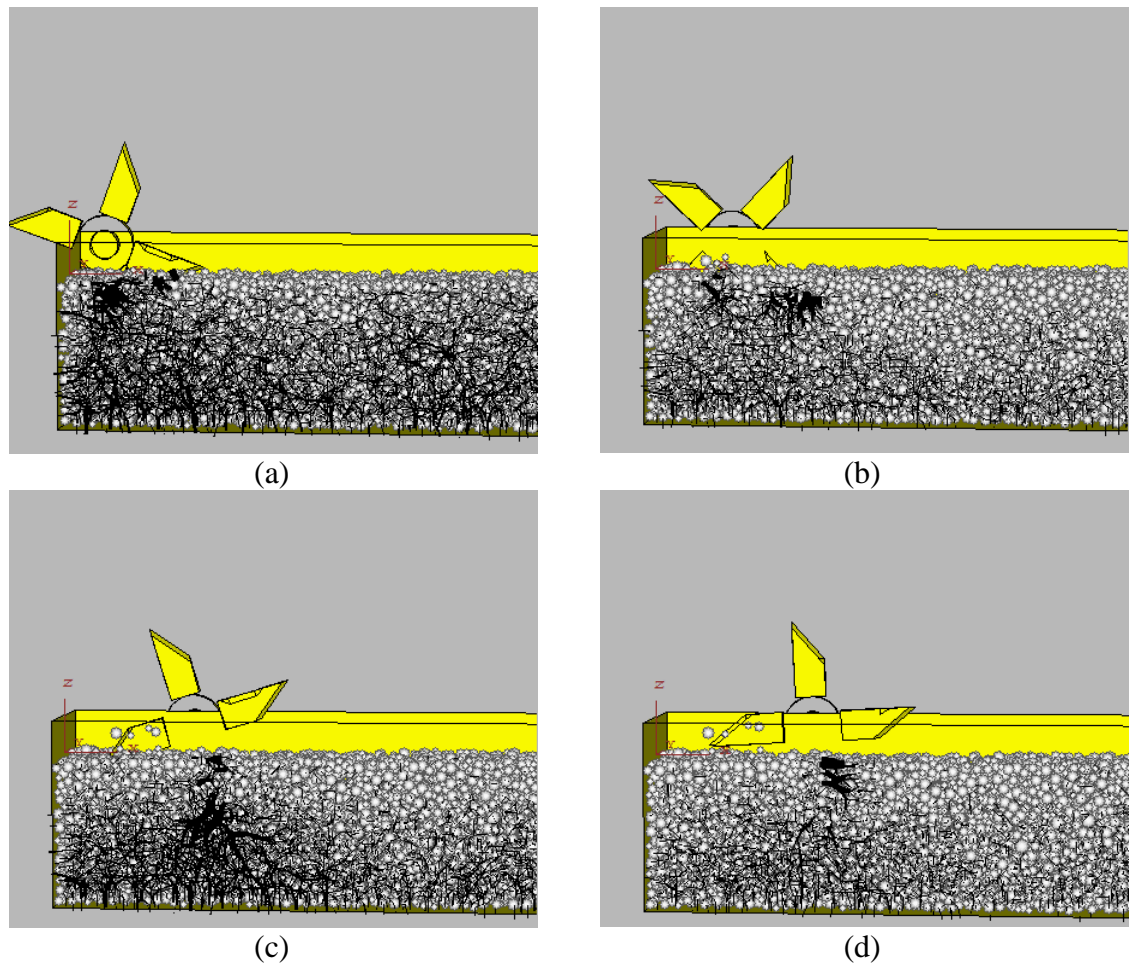


Figure 18: Screenshots of the soil-tool simulation over one shatter tine insertion from a) through d)

The simulated draft forces were validated with the draft forces predicted using Equation 6 for a zero swing angle and various working depths between 75-150 mm. The simulated draft force fluctuated over time. The maximum, minimum, and average values of the simulated draft force were recorded, and they were compared with those predicted using the regression equation (Figure 19). The model over predicted the draft force of the shatter tine at the depths of 75 to 100 mm, and under predicted draft force at the depths of 125 to 150 mm. However, the model fitted well within 100 – 150 mm with a relative error of 13.4-31.2%, which indicated that the model had a good correlation with the litera-

ture data. Overall, the simulated draft forces were within the variation range of the measurements.

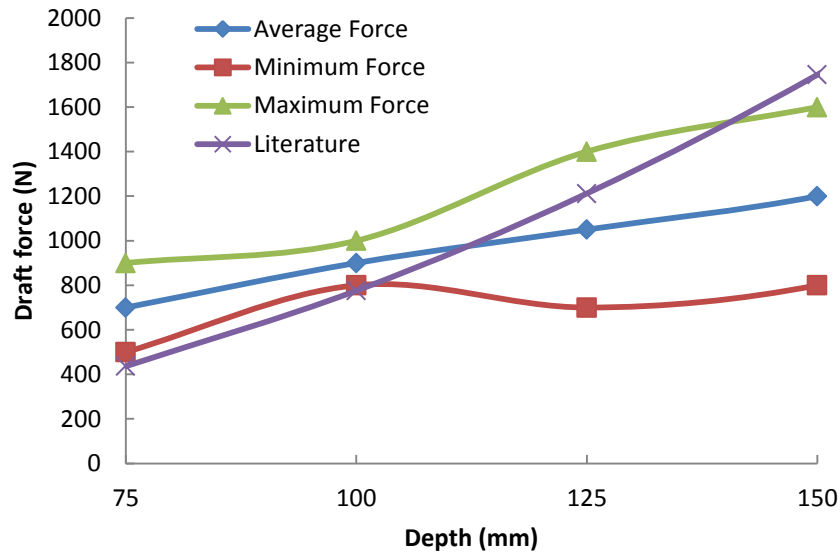


Figure 19: Simulated and literature values of draft forces at various working depths with 0° swing angle

3.4.3 Model Applications

There have been very few studies in the literature reporting measurements of vertical force for the shatter tine. Vertical force of a rolling tine is an important performance indicator as it is influenced by its working depth. In practice, machine ballasting has been always required to achieve penetration of rolling tines to a desired depth. Therefore, knowing the vertical force of the shatter tine will help select appropriate ballast and improve its field performance. The PFC^{3D} soil-tool model offered a method to predict the required vertical force at any working depth. Figure 20 is a typical curve of the simulated vertical force from the soil-tool interaction model for the depth of 150 mm. During the simula-

tion, four complete insertions of the shatter tines are shown by the four force peaks. Similar curves were found at different working depths, but with different peak magnitudes.

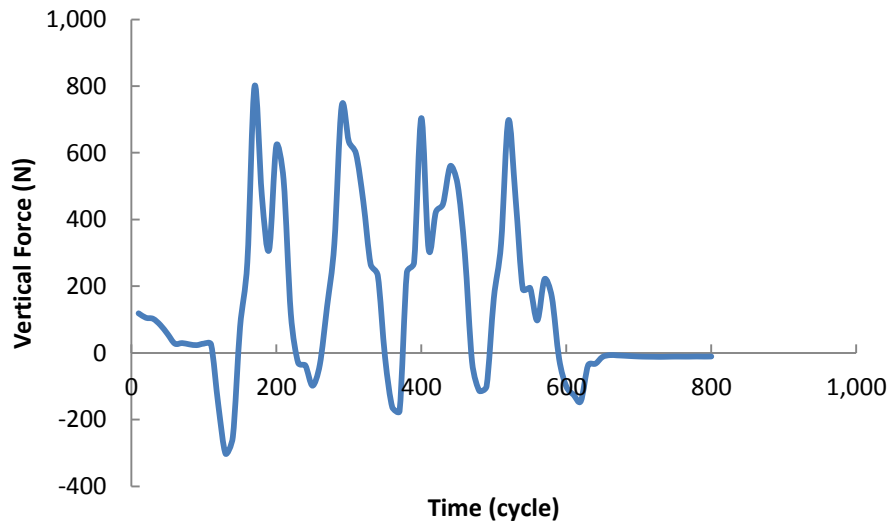


Figure 20: Sample of the simulated vertical force at 150 mm depth

The average peak vertical forces were obtained based on the maximum force measured from each of the four peaks, and the results are shown in Figure 21. The model predicts 350-700 N per shatter tine is required to puncture the silt loam soil. The vertical force increased in a linearly pattern until the maximum penetration force plateaus at 150 mm, but further investigations are required to validate these results. These results offered an indication of the possible results that may happen in the field and offer some assistance to any tool developer to ensure that the shatter tine are designed for such loads.

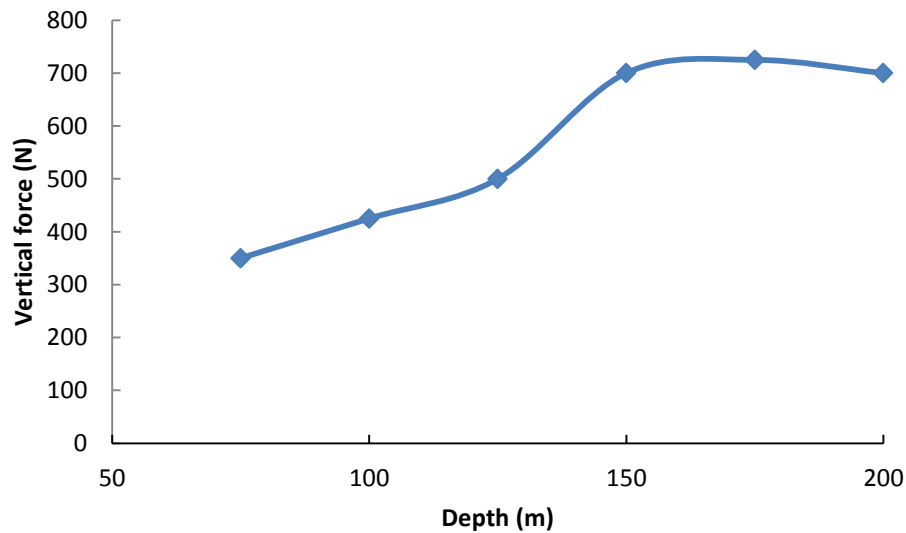


Figure 21: Simulated average vertical force of the shatter tine at different working depths at 0° swing angle

3.5 Conclusion

In this study, the soil-tool model was developed to offer a cost efficient method to study varying parameters without the extensive use of labour and equipment. The model was calibrated with field soil cone index data. From the model results, the calibrated soil was found to have a ball stiffness of 10 kN/m and bond stiffness of 1 kPa/m with a relative error of 7.7% for a silt loam soil. The model was capable of predicting the required draft to pull the shatter tine through the soil at various depths. As compared to literature data, the model performed well for 100 and 150 mm working depths where the corresponding relative errors were 13.4-31.2%. The model under predicted the draft at the greater depth and over predicted at the smaller depth. The soil-tool interaction model can also be used to predict the vertical force of shatter tine. However, the results of the vertical forces were not validated. The reasonable correlation between the simulations and literature data sug-

gested that DEM modeling is a very promising method to simulate highly variable soil properties, nonlinear dynamic behaviour of soil, and complex phenomena of soil-tool interaction.

3.6 Acknowledgements

Thanks are given to Mr. Song Ai, Mr. Mohammed Al-Amin Sadek, Mr. Majibur Rahman Khan Mr. Jinke Xu and Mr. Klayton Kaleta, for their help on field work.

3.7 References

- ASABE Standards, 2006. Procedures for Using and Reporting Data Obtained with the Soil Cone Penetrometer. ASAE EP542 FEB99: 1053-1055.
- Asaf, Z., Rubinstein, D. and I. Shmulevich. 2007. Determination of discrete element model parameters required for soil tillage. *Soil and Tillage Research* 92(2), 227-242.
- Bagherzadeh-Khalkhali, A. and A.A. Mirghasemi. 2009. Numerical and experimental direct shear tests for coarse-grained soils. *Particuology* 7: 83-91.
- Burlingame, M.J. 2008. Determination of aquifer and aquitard properties by inverse hydromechanical modeling. Continuum and Distinct Element Numerical Modeling in Geo-Engineering Paper No. 03-01 Minneapolis, MN: Itasca.
- Campbell, G.S. 1985. Soil Physics with Basic Transport Models for Soil-Plant Systems, Development in Soil Science 14. pp1-11. Elsevier, New York.
- Cundall, P.A. and O.D.L. Strack. 1979. A discrete numerical model for granular assemblies. *Geotechnique* 29: 47-65.
- Franco, Y., Rubinstein, D. and I. Shmulevich. 2007. Prediction of soil-bulldozer blade interaction using discrete element method. *Transaction of the ASABE* 50(2), 345-353.
- Godwin, R.J. 2007. A review of the effect of implement geometry on soil failure and implement forces. *Soil and Tillage Research* 97, 331-340.

- Itasca. 2008. PFC3D Particle Flow Code in 3 Dimensions, Theory and Background. Itasca Consulting Group, Inc. Minneapolis, Minnesota, USA.
- Landry, H., C. Laguë and M. Roberge. 2006. Discrete element modeling of machine–manure interactions. *Computers and Electronics in Agriculture* 52: 90 – 106.
- Lim, W.L. and G. McDowell. 2008. Discrete element modeling of kinematics of void collapse in granular materials. Continuum and Distinct Element Numerical Modeling in Geo-Engineering Paper No. 06-08 Minneapolis, MN: Itasca.
- Lu, M. and G. R. McDowell. 2007. The importance of modelling ballast particle shape in the discrete element method. *Granular Matter* 9:69–80.
- Lu, Z., S.C. Negi and J.C. Jofriet. 1997. A numerical model for flow of granular materials in silos. Part 1: model development. *Journal of Agricultural Engineering Research*. 68: 223-229.
- McLaughlin, N.B., Y.X. Li, S. Bittman, D.R. Lapen, S.D. Burt and B.S. Patterson. 2006. Draft requirements for contrasting liquid manure injection equipment. *Canadian Biosystems Engineering* 48: 2.29-2.37.
- McKyes, E. 1985. Soil Cutting and Tillage. Elsevier, New York.
- Momozu, M., A. Oida, M. Yamazaki and A.J. Koolen. 2003. Simulation of a soil loosening process by means of the modified distinct element method. *Journal of Terramechanics* 39: 207-220.
- Okunlola, A. and D. Payne. 1991. Use of force-deformation curves to estimate Young's modulus and its applications to soil aggregate breakdown. *Journal of Soil Science* 42, 543-549.
- Potyondy, D.O. and P.A. Cundall. 2004. A bond-particle model for rock. *International Journal of Rock Mechanics and Mining Science* 41(2004), 1392-1364.
- Potyondy, D.O. and J.F. Hazzard. 2008. Effects of stress and induced cracking on the static and dynamic moduli of rock. Continuum and Distinct Element Numerical Modeling in Geo-Engineering Paper No. 04-03 Minneapolis, MN: Itasca.
- Sakakibara, T., S. Kato, S. Shibuya and J.G. Chae. 2008. Effects of grain shape on mechanical behaviors and shear band of granular materials in DEM analysis. Continuum and Distinct Element Numerical Modeling in Geo-Engineering Paper No. 08-08 Minneapolis, MN: Itasca.
- Shamy, U.E. and T. Gröger. 2008. Micromechanical aspects of the shear strength of wet granular soils. *International Journal for Numerical and Analytical Methods in Geomechanics* 32: 1763-1790.

- Shen, J. and R.L. Kushwaha. 1998. Soil-Machine Interactions. New York, NY: Marcel Dekker Inc.
- Shmulevich, I., Rubinstein, D, and Z. Asaf. 2009. Discrete Element Modeling of Soil-Machine Interactions, in *Advances in Soil Dynamics*, Volume 3, Chapter 5, pp. 399-433 St. Joseph, MI: ASABE.
- Shmulevich, I. 2010. State of the art modeling of soil-tillage interaction using discrete element method. *Soil and Tillage Research* 111: 41-53.
- Starfield, A.M. 1997. A pragmatic approach to modeling for wildlife management. *Journal of Wildlife Management* 61(2): 261-270.
- Upadhyaya, S.K., Chancellor, W.J., Perumpral, J.V., Schafer, R.L., Gill, W.R., and G.E. VandenBerg. 1994. *Advances in Soil Dynamics*. Vol. 1. Chapter 2. ASAE Monograph Number 12, American Society of Agricultural and Biological Engineers.
- Van der Linde, J. 2007. Discrete Element Modeling of a Vibratory Subsoiler. Unpublished M.Sc. thesis. Department of Mechanical and Mechatronic Engineering, University of Stellenbosch, Matieland, South Africa.

General Conclusions

A step by step approach was used to evaluate the manure incorporation with the AerWay aerator and the feasibility of using PFC^{3D} to model soil behaviours. The objectives of this study was to experimentally determine the soil disturbances and manure distribution in soil, while creating a computer simulation model that simulates draft forces of the aerator. Although the treatment effects of tractor speed and manure application rate on the soil disturbance and manure distribution were not significantly different, the trends indicated that the faster tractor speeds would disturb more soil. Liquid manure, at application rate of 42 000 L/ha, reached a depth of 250 mm, and spread 200 mm in the forward direction and 100 mm in the lateral direction after one hour of application. The calibrated PFC^{3D} soil model was found to have a ball stiffness (k_n and k_s) of 10 kN/m and bond stiffness (\overline{K}_n and \overline{K}_s) of 1 kPa/m with a relative error of 7.7% for a silt loam soil. The model was able to predict draft and vertical forces of the aerator rolling tine. The model results on draft forces were in good agreement with the literature data at certain depths.

References

References

- Andreini, M.S. and T.S. Steenhuis. 1990. Preferential paths of flow under conventional and conservation tillage. *Geoderma* 46:85-102.
- ASAE Standards, 2004. Terminology and Definitions for Soil Tillage and Soil-Tool Relationships. ASAE EP291.2 FEB04: 114-118.
- Brebbia, C.A and L.C. Wrobel. 1980. The boundary element method. *Computer Methods in Fluids*: 26-48.
- Coetzee, C.J. and D.N.J. Els. 2009. Calibration of granular material parameters for DEM modelling and numerical verification by blade-granular material interactions. *Journal of Terramechanics* 46: 15-26.
- Georgison, R.R. 2010. Forces on a rotary tine aerator under normal working conditions. Unpublished M.Sc. thesis. Department of Agriculture and Bioresource Engineering, University of Saskatchewan, Saskatoon, SK.
- Holland, J.M.. 2004. The environmental consequences of adopting conservation tillage in Europe: reviewing the evidence. *Agriculture, Ecosystems and Environment* 103: 1-25.
- Landry, H. 2005. Numerical modeling of machine-product interactions in solid and semi-solid manure handling and land applications. Unpublished Ph.D. thesis Department of Agricultural and Bioresource Engineering, University of Saskatchewan, Saskatoon, SK.
- Nicolson, C.R., A.M. Starfield, G.P. Kofinas and J.A. Kruse. 2002. Ten heuristics for interdisciplinary modeling projects. *Ecosystem* 5: 376-384.
- Nissani, M. 1997. Ten cheers for interdisciplinary: the case for interdisciplinary knowledge and research. *Social Science Journal* 34(2): 210-216.
- Oreskes, N., K. Shrader-Frechette and K. Belitz. 1994. Verification, validation, and confirmation of numerical models in the earth sciences. *Science* 263: 641-646.

- Schwartz, F.W. and H. Zhang. 2002. Theory of ground-water flow. In *Fundamentals of Ground Water*, 96-127. New York, NY: John Wiley and Sons, Inc.,
- Shmulevich, I. 2010. State of the art modeling of soil-tillage interaction using discrete element method. *Soil and Tillage Research* 111: 41-53.
- Starfield, A.M. 1997. A pragmatic approach to modeling for wildlife management. *Journal of Wildlife Management* 61(2): 261-270.
- Tijskens, E., H. Amon and J. De Baerdemaeker. 2003. Discrete element modeling for process simulation in agriculture. *Journal of Sound and Vibration*. 266(3): 493-514.

